CORRECTED 3 FEBRUARY 2021, SEE ERRATUM

SCIENCE TRANSLATIONAL MEDICINE | RESEARCH ARTICLE

PRETERM BIRTH

Enhanced drug delivery to the reproductive tract using nanomedicine reveals therapeutic options for prevention of preterm birth

Hannah C. Zierden[1,2], Jairo I. Ortiz[1,3], Kevin DeLong[1,3], Jingqi Yu[1,4], Gaoshan Li[1,2], Peter Dimitrion[1], Sabrine Bensouda[1], Victoria Laney[1,2], Anna Bailey[1,4], Nicole M. Anders[5], Morgan Scardina[5], Mala Mahendroo[6], Sam Mesiano[7], Irina Burd[8], Gunter Wagner[9], Justin Hanes[1,2,3,4,5], Laura M. Ensign[1,2,3,4,5,8]*

Inflammation contributes to nearly 4 million global premature births annually. Here, we used a mouse model of intrauterine inflammation to test clinically used formulations, as well as engineered nanoformulations, for the prevention of preterm birth (PTB). We observed that neither systemic 17α-hydroxyprogesterone caproate (Makena) nor vaginal progesterone gel (Crinone) was sufficient to prevent inflammation-induced PTB, consistent with recent clinical trial failures. However, we found that vaginal delivery of mucoinert nanosuspensions of histone deacetylase (HDAC) inhibitors, in some cases with the addition of progesterone, prevented PTB and resulted in delivery of live pups exhibiting neurotypical development. In human myometrial cells in vitro, the P4/HDAC inhibitor combination both inhibited cell contractility and promoted the anti-inflammatory action of P4 by increasing progesterone receptor B stability. Here, we demonstrate the use of vaginally delivered drugs to prevent intrauterine inflammation–induced PTB resulting in the birth of live offspring in a preclinical animal model.

INTRODUCTION

It was estimated that the yearly economic burden of preterm birth (PTB) tops $26 billion in the United States alone (*1*, *2*). Around 15 million babies are born preterm each year, making PTB the largest contributor to infant mortality and morbidity worldwide (*3*, *4*). The only U.S. Food and Drug Administration (FDA)–approved therapy for the prevention of PTB is an intramuscular injection of the synthetic progestin 17α-hydroxyprogesterone caproate (17-OHPC; Makena). However, a recent randomized double-blind controlled trial demonstrated that Makena failed to decrease PTB rates in women with a history of spontaneous PTB and had no impact on fetal morbidity (*5*). In response, the FDA's Center for Drug Evaluation and Research (CDER) has issued a recommendation that Makena be withdrawn from the market, which would leave the field with no approved prophylaxes for PTB (*6*–*9*).

Vaginal progesterone (P4) gel (Crinone) is used off-label to prevent premature delivery in women with a sonographic short cervix (*10*). Vaginally administered drugs are optimal for targeting the female reproductive tract, because they are preferentially transported to the uterus before reaching the systemic circulation as a result of countercurrent exchange between the vaginal veins and uterovaginal arteries or lymphatic vessels, via the uterine first-pass effect (*11*). However, vaginal drug administration must be engineered to effectively overcome the cervicovaginal mucus (CVM) that protects the female reproductive tract. Mucus is the primary barrier to drug absorption and retention, and the physiology and structure of the various epithelial surfaces further limit effective drug delivery (*12*, *13*). We have previously demonstrated that water absorption induced by hypotonic vehicles increases the vaginal distribution of mucoinert nanoparticles (*12*) and that these formulations can enhance mucosal absorption of poorly soluble drugs (*14*, *15*). We previously showed that our mucoinert P4 nanosuspension (NS) was more effective than Crinone gel in preventing PTB in a model of P4 withdrawal (*15*). Both 17-OHPC and Crinone have shown varied efficacy in clinical trials, as well as in preclinical animal studies (*10*, *16*), highlighting the critical need for better understanding of how drug action in vivo, formulation, and route of drug administration play a role in the effective prevention of PTB.

Inflammation and infection account for 25 to 40% of all PTBs with intact membranes (*4*) and 20 to 30% of cases of preterm premature rupture of membranes (*17*). In addition, inflammation and infection can lead to fetal inflammatory response syndrome, which is associated with fetal brain injury (*18*). However, progestin supplementation in the context of inflammation is controversial (*19*–*22*). Although systemic P4 concentrations steadily increase over the course of normal human gestation (*23*, *24*), P4 is known to have different functional roles mediated by the two predominant progesterone receptor (PR) isoforms A and B (*25*–*27*). PRB, which is more dominant in early pregnancy, promotes the anti-inflammatory action of P4 and maintains uterine quiescence (*28*, *29*). Conversely, the ratio of PRA to PRB increases in the myometrium over the course of pregnancy, facilitating a switch in P4 action (*28*, *29*). PRA decreases the myometrium's sensitivity to the anti-inflammatory actions of P4 and helps coordinate contractions (*30*). Normal term labor is inherently a proinflammatory process enabled by this

[1]Center for Nanomedicine, Wilmer Eye Institute, Johns Hopkins University School of Medicine, Baltimore, MD 21231, USA. [2]Department of Chemical and Biomolecular Engineering, Johns Hopkins University, Baltimore, MD 21218, USA. [3]Department of Ophthalmology, Wilmer Eye Institute, Johns Hopkins University School of Medicine, Baltimore, MD 21231, USA. [4]Department of Biomedical Engineering, Johns Hopkins University School of Medicine, Baltimore, MD 21231, USA. [5]Sidney Kimmel Comprehensive Cancer Center, Johns Hopkins University School of Medicine, Baltimore, MD 21287, USA. [6]Department of Obstetrics and Gynecology, University of Texas Southwestern Medical Center, Dallas, TX 75390, USA. [7]Department of Reproductive Biology, Case Western Reserve University, Cleveland, OH 44106, USA. [8]Integrated Research Center for Fetal Medicine, Department of Gynecology and Obstetrics, Johns Hopkins University, Baltimore, MD 21287, USA. [9]Department of Ecology and Evolutionary Biology, Yale University, New Haven, CT 06520, USA.
*Corresponding author. Email: lensign@jhmi.edu

functional P4 withdrawal, and proinflammatory stimuli have been shown to similarly enhance the stability of PRA (*30*). Thus, P4 supplementation would not have a therapeutic benefit in the setting of inflammation-induced PTB, potentially explaining the limited clinical success.

Murine models of inflammation-induced PTB have been used to assess therapeutic efficacy in preventing PTB and mitigating neurological deficits in offspring (*18*, *31*–*34*). One of the more common animal models involves intrauterine injection of lipopolysaccharide (LPS) on embryonic day 15 of 19 (E15) or later term on E17 (*32*, *35*, *36*). Prior studies examining systemic progestins for preventing inflammation-induced PTB described maintenance of in utero fetal viability at 8 to 24 hours after injection on E15 but either did not evaluate birth outcomes or reported that no live pups reached full term (*34*, *37*, *38*). Similarly, systemic pretreatment (PT) with P4 did not alter the PTB rate with later-term (E17) intrauterine LPS exposure (*32*). Here, using our recently described murine model of intrauterine LPS injection (*39*), we show that P4 alone does not prevent inflammation-induced PTB. Further, in some cases, P4 actually worsened outcomes, supporting the idea that P4 alone may not be suitable for therapeutic use in inflammation-induced PTB.

Histone deacetylase (HDAC) inhibitors have been studied preclinically for use in a variety of inflammatory disorders and have been studied in the context of parturition (*40*–*43*). It has been observed that histone deacetylation increases at term in the myometrium (*43*) and in the cervix (*44*, *45*). Here, we present findings using HDAC inhibitors for the prevention of PTB in a preclinical murine model. We engineered mucoinert NS of both P4 and two HDAC inhibitors and showed that HDAC inhibitors, both with and without P4 supplementation, reduced PTB rates, leading to delivery of live, neurotypical offspring. Systemic delivery of the same drugs had no effect on PTB rate. Using human myometrial cells, we demonstrate that the P4/HDAC inhibitor combination resulted in a shift in PR ratio, promoting PRB expression, which supports the anti-inflammatory action of P4. Further, the P4/HDAC inhibitor combination suppressed human myometrial cell contractility in vitro when incubated at the drug concentrations measured in mouse myometrial tissue after vaginal dosing in vivo. These results highlight the utility of nanomedicine-based drug delivery strategies for increasing our understanding of the processes that lead to inflammation-induced PTB and developing therapeutic strategies for prevention.

RESULTS

Clinically used progestin therapies do not prevent inflammation-induced PTB in a murine model

We first sought to test the only FDA-approved drug for the prevention of PTB, systemic 17-OHPC, in our murine model of inflammation-induced PTB. As described in our recent publication, we adapted the intrauterine LPS injection model to use double distal injections (DDIs), which increased uniformity of the inflammatory stimulus, increased expression of contractility genes in the myometrium, led to a linear dose response, and increased PTB induction rates, as compared to the single proximal injection (SPI) model (*39*). Dams were given intrauterine injections of 20 μg of LPS and treated systemically with 80 μg of 17-OHPC (Makena), resulting in 87.5% PTB (n = 7 of 8) compared to 90% PTB (n = 27 of 30) in the LPS control group (Fig. 1A). We previously demonstrated that formulating P4 for increased local vaginal drug absorption and delivery to the reproductive tract tissues via the uterine first-pass effect led to more effective prevention of PTB in the mifepristone (RU486) model of P4 withdrawal (*15*). Given the anti-inflammatory effects of P4, we next sought to test the hypothesis that improved P4 delivery to the reproductive tract would lead to more effective prevention of inflammation-induced PTB. We tested the vaginal P4 gel (Crinone) at the same dose that showed some therapeutic effect in the RU486 model, 8 mg, but all of the animals were delivered preterm (100% PTB, n = 6 of 6), compared to 90% PTB in the LPS control group (Fig. 1A) (*15*). To rule out the possibility that the LPS induction was too severe, we next tested these clinical formulations after injections of 15 μg (Fig. 1B) and 5 μg (Fig. 1C) of LPS. Similarly, no therapeutic effect on the PTB rates was observed at 15 μg of LPS (73% PTB, n = 11 of 15) for P4 gel (100% PTB, n = 7 of 7) or at 5 μg of LPS (38% PTB, n = 5 of 13) for either 17-OHPC injection (50% PTB, n = 5 of 10) or P4 gel (50% PTB, n = 5 of 10). The saline sham control (0 μg of LPS) had 0% PTB (n = 0 of 20) as expected; however, dosing 8 mg of vaginal P4 gel to saline sham–treated mice led to 55% PTB (n = 6 of 11) (Fig. 1D).

Vaginal progesterone alone is insufficient for preventing inflammation-induced PTB in a murine model

We previously observed that a single vaginal treatment of Crinone gel in pregnant mice led to local inflammation, likely due to the hypertonic excipients (*15*, *46*), and thus thought that it was possible that the local inflammation caused by Crinone gel could be contributing to the PTB phenotype. In addition to providing increased P4 delivery to reproductive tract tissues, we previously found that our mucoinert P4 NS did not cause notable inflammation or toxicity with vaginal dosing (*15*). To perform dose ranging experiments, we formulated P4 NS at 5, 25, 50, 80, and 250 mg/ml (Table 1 and Fig. 2). Similar to what we previously described (*15*), P4 was stabilized with 2 to 6% F127 in water and nanomilled in a 2.0-ml Eppendorf tube with 1.5 to 3.5 g of zirconium oxide–stabilized homogenization beads (ZROB05) for 10 hours. Size was checked over the course of 10 hours of nanomilling to minimize size and polydispersity index (PDI). For all formulations, diameter (gray bars in Fig. 2A) decreased over the course of 10 hours, leading to final formulations in the range of 300 to 380 nm to allow effective mucus penetration. PDIs (white dots in Fig. 2A) were between 0.10 and 0.25, indicating relative homogeneity in nanoparticle size. The ζ-potential (black bars in Fig. 2A) values were between −2.5 and 0.0 mV (Table 1). The physicochemical properties of the P4 NS (50 mg/ml) over the course of 10 hours of milling are shown in Fig. 2A. Again, working with the 20 μg of LPS induction, we tested four different doses of vaginal P4 NS (100 μg, 100% PTB, n = 5 of 5; 500 μg, 88% PTB, n = 7 of 8; 1 mg, 85% PTB, n = 17 of 20; and 5 mg, 100% PTB, n = 5 of 5) as shown in Fig. 2B. In no case did the treatment have an effect on the PTB rate. Because of the lack of PTB prevention with P4 dosing after LPS challenge, we then tested whether P4 PT would be more effective in preventing inflammation-induced PTB. Dams were given 8 mg of P4 on the mornings of E13 and E14. On E15, dams were challenged with 20 μg of LPS and given another dose of 8 mg of P4, resulting in 100% PTB (n = 6 of 6) (Fig. 2C).

Progesterone combined with trichostatin A prevents inflammation-induced PTB when dosed vaginally in a murine model

It was previously shown that systemic administration of trichostatin A (TSA), a potent HDAC inhibitor, delayed normal term delivery in

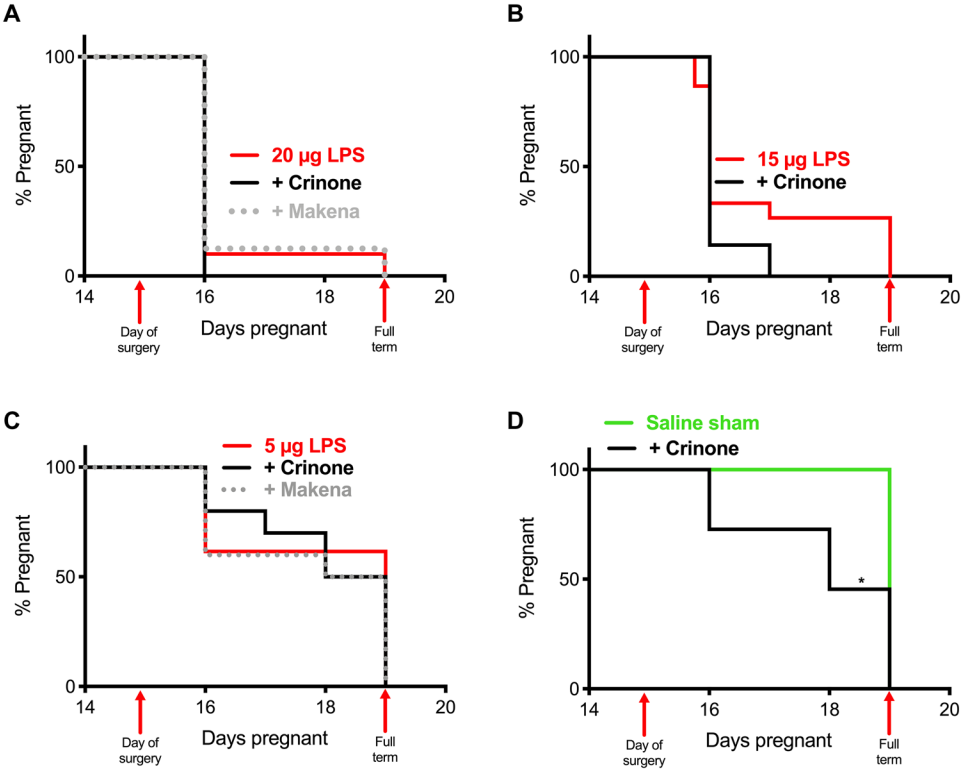

Fig. 1. PTB prevention with clinical treatments. Pregnancy survival curves showing the percentage of animals remaining pregnant after DDI of LPS on E15. (**A**) Daily intraperitoneal injection of Makena (17-OHPC) (80 µg, $n = 8$) or vaginal administration of Crinone (8 mg, $n = 6$) compared to 20 µg of LPS alone ($n = 10$). (**B**) Daily vaginal administration of Crinone ($n = 7$) compared to 15 µg of LPS alone ($n = 15$). (**C**) Daily intraperitoneal injection of Makena ($n = 10$) or vaginal administration of Crinone ($n = 10$) compared to 5 µg of LPS alone ($n = 13$). (**D**) Daily vaginal administration of Crinone ($n = 11$) compared to saline sham ($n = 20$) (*$P = 0.0002$, Mantel-Cox test).

mice (*43*). It has also been suggested that a decrease in histone acetylation at term may affect PR function supportive of the anti-inflammatory activity of P4 (*43*, *47*). Thus, we hypothesized that combining TSA with P4 may improve the therapeutic action of P4 in inflammation-induced PTB. We sought to formulate a TSA NS with physicochemical properties appropriate for improved mucosal distribution and vaginal drug absorption. Table S1 details the iterations of tube size, bead mass, F127 concentration, and concentration of additional stabilizers (HS15, F68, or TPGS) tested. A final TSA formulation was identified as having the optimal combination of physical characteristics, including low size, low PDI, near-neutral ζ-potential, and reproducibility between batches (table S1). The final TSA NS was formulated using 4% F127 in a 1.5-ml Eppendorf tube, with 1.5 g of 0.5-mm zirconium silicate–stabilized homogenization beads (ZSB05) with a concentration of 1.5 mg/ml of TSA (Table 1). The physicochemical properties of the final TSA NS as a function of milling time are shown in Fig. 3A. NS diameter (gray bars in Fig. 3A) and PDI (white dots in Fig. 3A) generally decreased over the course of 10 hours of milling time (Fig. 3A). We then performed P4 NS dose ranging experiments in combination with the TSA NS. As shown in fig. S1, the vaginal P4/TSA NS combination was effective in preventing LPS-induced PTB at several P4 NS doses. We then compared the efficacy of vaginal administration of P4/TSA NS (1 mg/15 µg) compared to either drug alone. As shown in Fig. 3B, P4 NS was ineffective with 85% PTB ($n = 17$ of 20) compared to 90% PTB ($n = 27$ of 30) in the LPS control group. The PTB rate for the TSA NS group was 70% ($n = 14$ of 20). The combination of P4/TSA NS reduced the PTB rate to 60% ($n = 12$ of 20; $P = 0.003$). We then repeated the experiment to compare vaginal administration of the P4/TSA NS to systemic administration at the same dose. In this experiment, vaginal administration of P4/TSA NS resulted in 50% PTB ($n = 4$ of 8), whereas equivalent doses of P4/TSA NS given by intraperitoneal injection resulted in 87.5% PTB ($n = 7$ of 8) (Fig. 3C). Vaginal administration significantly prevented PTB in the LPS-induced murine model compared to systemic administration ($P = 0.048$) (Fig. 3C). In the vehicle control study, 30 µl of 4% F127 (w/v) showed no difference in PTB rate (83%, $n = 5$ of 6), as compared to the LPS control (fig. S2).

Vaginal drug NS combination treatment leads to delivery of live pups that exhibit neurotypical development

Pup viability was calculated for each litter as a percentage relative to the number of viable pups in utero on E15 for litters born to dams after treatment with P4 NS, TSA NS, and P4/TSA NS (Fig. 3D). This viability measure is useful for comparison, as we have seen CD-1 litters on E15 ranging in size from 6 to 19 pups (fig. S3). When calculating the average pup viability, litters that were delivered prematurely were not included because the viability was 0% at all degrees of prematurity. We observed that vaginal treatment with either TSA NS or P4/TSA NS significantly increased average pup viability in litters compared to the LPS control group ($P < 0.001$ and $P = 0.0021$, respectively) (Fig. 3D). Individual litter viability is shown in fig. S4.

Exposure to inflammation in utero can lead to neurological deficits (*3*, *18*, *36*), so we next sought to analyze the neurological development of pups born after vaginal P4/TSA NS treatment to prevent inflammation-induced PTB. It has been shown that an increased brain weight percentage is indicative of delayed neurological development (*48*). We collected pup brains on postnatal day (PND) 22 and measured their weight as a percentage of the pup body weight. As shown in Fig. 3E, there was no difference in the brain weight percentages for either male or female pups after treatment with P4/TSA NS compared to the pups from dams receiving saline sham surgery. In addition, we performed behavioral tests to gauge the neurological development of offspring. The LPS control group had very low rates of term delivery (Fig. 3B) and low fetal viability (Fig. 3D and fig. S4), so we compared pups in the treatment group to the unexposed pups in the saline sham group. Figure 3 shows results for cliff aversion (Fig. 3F), negative geotaxis (Fig. 3G), and surface righting tests (Fig. 3H), as well as the time spent in center (Fig. 3I), distance

Table 1. NS physical properties. P4, TSA, and SAHA NS formulations and sizes. Particles were formulated via wet milling (10 hours) in Pluronic F127. Size, PDI, and ζ-potential are represented as means ± SD ($n \geq 3$).

Drug concentration	% F127 (w/v)	Beads type-mass (g)	Tube size (ml)	Size (nm)	PDI	ζ-Potential (mV)
P4 (5 mg/ml)	2	ZROB05 (1.5)	2.0	346.4 ± 15.8	0.11 ± 0.07	−1.08 ± 0.84
P4 (25 mg/ml)	2	ZROB05 (2.4)	2.0	302.5 ± 9.7	0.17 ± 0.02	−1.59 ± 0.21
P4 (50 mg/ml)	2	ZROB05 (2.4)	2.0	305.9 ± 5.8	0.21 ± 0.15	−0.087 ± 0.012
P4 (80 mg/ml)	2	ZROB05 (2.4)	2.0	376.7 ± 14.1	0.19 ± 0.12	−0.92 ± 0.72
P4 (250 mg/ml)	6	ZROB05 (3.5)	2.0	315.5 ± 7.9	0.17 ± 0.06	−1.48 ± 0.17
TSA (1.5 mg/ml)	4	ZSB05 (1.5)	1.5	215.9 ± 12.9	0.12 ± 0.07	−0.06 ± 0.04
SAHA (1.5 mg/ml)	4	ZROB05 (1.5)	1.5	263.5 ± 48.6	0.37 ± 0.24	−2.44 ± 0.89

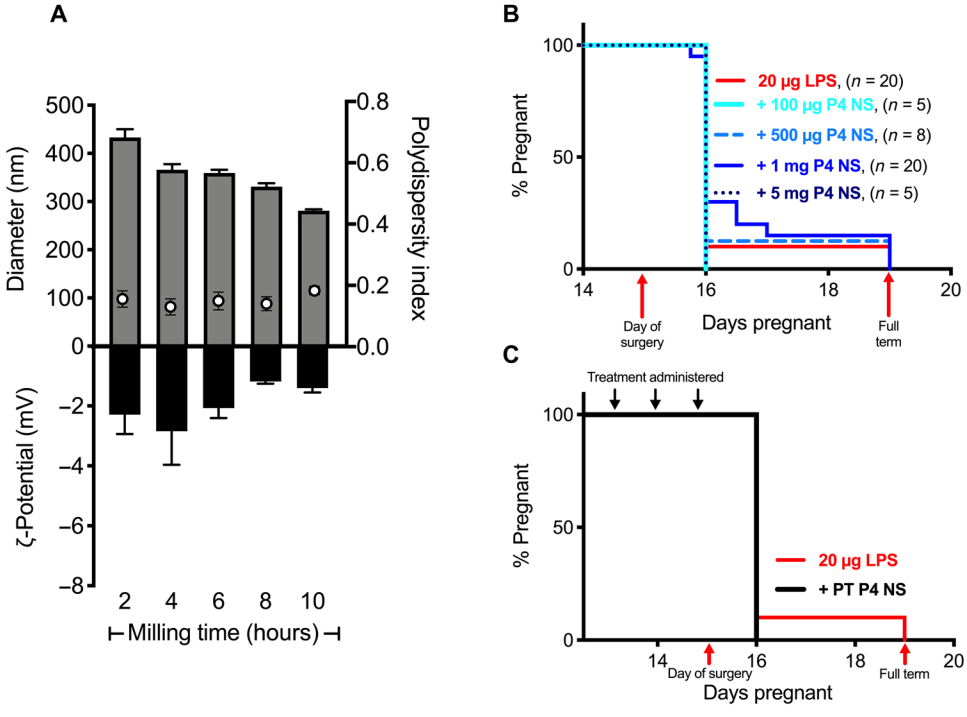

Fig. 2. PTB prevention with P4 NS treatments. (**A**) Diameter (gray bars), PDI (white dots), and ζ-potential (black bars) of P4 NS (50 mg/ml) over 10 hours of nanomilling. Data are represented as means ± SEM ($n \geq 3$). (**B**) Pregnancy survival curves showing the percentage of animals remaining pregnant after DDI of LPS on E15. Daily vaginal administration of various doses of P4 NS compared to 20 μg of LPS alone ($n = 20$). (**C**) Daily PT with vaginal administration of 8 mg of P4 NS starting on E13 ($n = 6$) compared to 20 μg of LPS alone ($n = 10$).

traveled (Fig. 3J), and average velocity (Fig. 3K) for pups during the open field test. Pups that failed a given task were excluded. In Fig. 3G, only one pup from the P4/TSA NS group passed the negative geotaxis test on PND 5. Failure rates were similar across groups and decreased with increasing age (table S2). There were no differences between saline sham and the P4/TSA NS group for any tests performed on any of the test days (PNDs 9, 13, 15, 17, and 22) (Fig. 3, F to K). Decreased endotoxin content in the amniotic fluid was observed in the all three treatment groups compared to the LPS control group 8 hours after LPS exposure ($P = 0.001$) (fig. S5).

Vaginally administered TSA localizes and rapidly converts to active metabolites in reproductive tract tissues

We have previously investigated the pharmacokinetics (PK) of P4 when dosed vaginally (*15*). We compared the PK of 8 mg of P4 when given as a gel (Crinone) or as an NS and showed that NS provided an increased area under the curve (AUC) in the plasma, cervix, and uterine tissues (*15*). Here, we dosed the P4/TSA (1 mg/15 μg) NS combination to assess the drug localization in the reproductive tract tissues. As shown in Fig. 4, we saw similar double peaks in P4 in plasma and myometrium around ~1 and ~4 hours due to recirculation after uterine first pass, as described previously (*11*, *15*, *49*). For TSA, peak concentrations in all compartments were observed at the earliest time point sampled (1 hour) and rapidly declined thereafter, consistent with prior studies describing the metabolism of TSA to active metabolites in vivo (*50*). TSA concentrations were undetectable after 1 hour in the distal myometrium, 2 hours in the proximal myometrium, and 6 hours in the plasma (Fig. 4). TSA concentrations declined but were still measurable in the cervical tissue for the full 12-hour time course, likely because the starting concentrations were much higher from the direct exposure to the NS (Fig. 4B). Figure S6 shows approximate concentrations of active metabolites of TSA analyzed using previously described methods (*50*). In the proximal myometrium, *N*-demethyl TSA amide and *N*-demethyl TSA acid showed a first peak at 1 hour, with a recirculation second peak around 3 hours, indicative of uterine first-pass metabolism (fig. S6). We also dosed P4 NS (1 mg) alone to determine whether TSA had an effect on P4 metabolism (fig. S7). There was no difference in the P4 AUC for the plasma, cervix, distal, or proximal myometrial tissue (fig. S8).

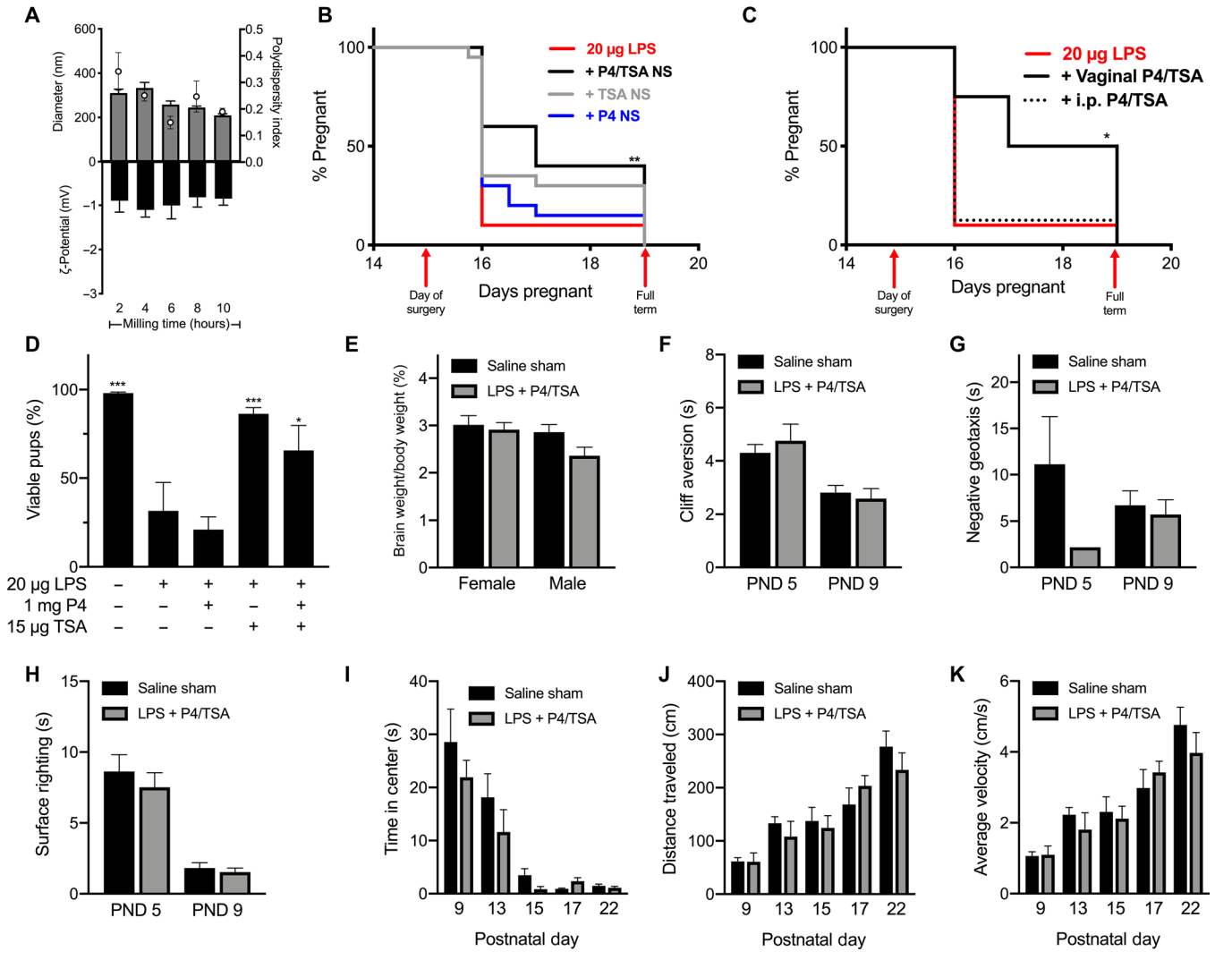

Fig. 3. PTB prevention and behavioral analyses for P4/TSA treatments. (**A**) Diameter (gray bars), PDI (white dots), and ζ-potential (black bars) of TSA NS (1.5 mg/ml) over 10 hours of nanomilling. Data are represented as means ± SEM ($n \geq 3$). (**B**) Pregnancy survival curves showing the percentage of animals remaining pregnant after DDI of 20 µg of LPS on E15. Daily vaginal administration of P4 NS (1 mg, $n = 20$; repeated from Fig. 2B), TSA (15 µg, $n = 20$), or P4/TSA NS (1 mg/15 µg, $n = 20$) compared to LPS alone ($n = 30$) (**$P = 0.003$, Mantel-Cox test). (**C**) Daily vaginal administration of P4/TSA ($n = 8$) or intraperitoneal (i.p.) injection of P4/TSA NS (1 mg/15 µg, $n = 8$) compared to LPS alone ($n = 10$). Vaginal administration significantly reduced PTB rates compared to intraperitoneal injection (*$P = 0.048$) and LPS alone ($P = 0.024$). (**D**) For term litters, percentage of pups born live compared to viable pups counted on E15. *$P < 0.05$ and ***$P < 0.001$ compared to LPS. (**E**) Pup brain weight as a percentage of body weight for pups from the saline sham group or 20 µg of LPS + P4/TSA on PND 22. (**F** to **K**) Behavioral tests for pups in the saline sham or 20 µg of LPS + P4/TSA group: (F) cliff aversion, (G) negative geotaxis, (H) surface righting, (I) time in center for open field, (J) distance traveled in open field, and (K) average velocity in open field. Failures were not included in data analysis and are presented in table S2. Data are shown as means ± SEM ($n \geq 3$).

Prevention of inflammation-induced PTB was associated with changes in myometrial gene expression

When characterizing our adapted LPS model, we observed an increase in expression of genes related to myometrial contractility (*39*). Here, we evaluated the effect of a single vaginal dose of P4 NS, TSA NS, and P4/TSA NS on expression of markers of inflammation in the myometrium 8 hours after LPS injection. It is worth noting, though, that more variability is expected in the treatment groups because each group contains dams that would go on to deliver preterm and dams that would not. As shown in Fig. 5A, the 20-µg LPS dose significantly increased myometrium interleukin-6 (*Il6*) expression 14-fold compared to the saline sham group ($P < 0.0001$), consistent with prior demonstration of increased expression at time of labor (*51*). All treatment groups showed a significant decrease in *Il6* expression, as compared to the LPS group ($P = 0.0008$ for P4, $P = 0.0011$ for TSA, and $P = 0.0035$ for P4/TSA) (Fig. 5A). Similarly, *Il1*β was significantly up-regulated threefold in the LPS group compared to the saline sham group ($P = 0.035$) (Fig. 5B), consistent with what was previously described in inflammation-induced PTB (*35*, *52*). None of the treatment groups showed differences in *Il1*β expression compared to the LPS group (Fig. 5B). Nuclear factor κ-light-chain-enhancer (*Nfκb1*) in activated B cells mediates the inflammatory response and plays a role in the onset of parturition (*53*). LPS alone resulted in a 4.2-fold increase in myometrial expression

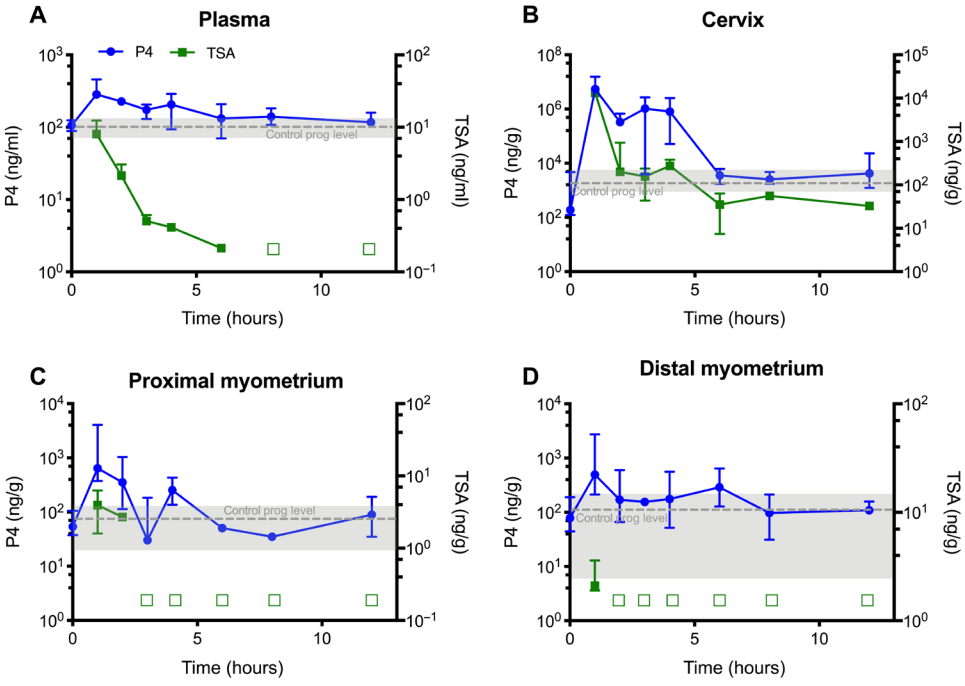

Fig. 4. PK for P4/TSA treatment. P4 (left axis) and TSA (right axis) concentrations in (**A**) plasma, (**B**) cervical tissue, (**C**) proximal myometrial tissue, and (**D**) distal myometrial tissue collected from healthy dams after a single vaginal P4/TSA NS dose on E15. An empty square symbol indicates that TSA concentrations in all samples were below the lower limit of quantification (0.2 ng/ml or ng/g) at that time point. Gray dashed lines represent mean endogenous concentrations of P4 from untreated healthy E15 dams. Data are presented as median ± interquartile range ($n = 3$).

of *Nfκb1* compared to the saline sham ($P < 0.0001$) (Fig. 5C). Relative *Nfκb1* expression (with respect to the saline group) was 1.52 for the P4 NS group ($P < 0.0001$ compared to LPS), 1.54 for the TSA NS group ($P < 0.0001$ compared to LPS), and 1.49 for the P4/TSA group ($P < 0.0001$ compared to LPS) (Fig. 5C). Chemokine ligand 3 (*Ccl3*) is overexpressed in uterine tissues near the time of labor (*54*). Tissue from the LPS group showed a sixfold increase in *Ccl3* expression compared to the saline sham group ($P = 0.0024$) (Fig. 5D). The TSA NS and P4/TSA NS groups showed a significant ~2.2-fold reduction in *Ccl3* expression compared to the LPS group ($P = 0.027$ and $P = 0.04$, respectively) (Fig. 5D). Cyclooxygenase-2 (*Cox2*) expression occurs upstream of myometrial contractions (*52*, *55*, *56*). We observed a 13-fold increase in *Cox2* expression in myometrial tissue from the LPS induction group compared to the saline sham ($P = 0.0002$) (Fig. 5E). The TSA NS group showed the largest decrease compared to the LPS group (6.5-fold; $P = 0.0009$), with the P4 NS–treated group decreased 3-fold ($P = 0.013$) and the P4/TSA NS group decreased 3.8-fold ($P = 0.004$) (Fig. 5E).

We also investigated how the expression of contractile genes was affected by vaginal drug treatment. Connexin-43 (*Cx43*) regulates smooth muscle contractions in the myometrium (*52*). As shown in Fig. 5F, the LPS induction group showed a 1.7-fold increase in *Cx43* expression compared to the saline sham group ($P = 0.002$). All treatment groups showed decreased *Cx43* expression compared to the LPS group, with the P4/TSA group showing the largest average decrease (2.5-fold; $P < 0.0001$) (Fig. 5F). Oxytocin receptor (*Oxtr*) increases uterine responsiveness to contractile signals (*57*). The LPS induction group showed a twofold increase in *Oxtr* expression compared to the saline sham group ($P = 0.13$) (Fig. 5G). The P4 treatment group was not different from the LPS group, whereas the P4/TSA group showed a significant 2.8-fold decrease in *Oxtr* expression compared to the LPS group ($P = 0.03$) (Fig. 5G). Zinc finger E-box–binding homeobox 1 (*Zeb1*) has been shown to regulate uterine quiescence in response to P4 (*57*). At the time of labor, *Zeb1* expression decreases (*57*). There were no differences between groups when looking at *Zeb1* expression (Fig. 5H). Last, we investigated changes in expression of steroid 5α reductase type 1 (*Srd5a1*), which is involved in P4 metabolism (*58*). Similar to what others have observed in the cervix, the expression of *Srd5a1* was down-regulated in myometrial tissue from LPS-treated mice as compared to the saline group ($P = 0.048$) (Fig. 5I) (*58*). There were no differences in *Srd5a1* expression among treatment groups (Fig. 5I).

Figure S9 shows the expression of genes that were previously shown to be altered in the cervical tissue in mouse models of inflammation-induced PTB, as well as in term labor (*58*, *59*). However, we did not observe differences in gene expression in the cervical tissue due to intrauterine LPS DDI compared to saline sham (fig. S9). Thus, despite high drug concentrations in the cervical tissue, we found few differences in the expression of these genes with vaginal drug treatment. There were no differences in *Il6*, *Cx43*, or matrix metalloproteinase 8 (*Mmp8*) expression. The TSA-treated group showed significant up-regulation of *Cox2*, as compared to the saline control group ($P = 0.005$) (fig. S9B). The P4-treated group showed significant down-regulation of a disintegrin-like and metalloproteinase with thrombospondin type 1 motif (*Adamts1*), as compared to the saline control group ($P = 0.02$) (fig. S9E).

P4/TSA combination alters PR ratios in human myometrial cells in vitro

We next investigated how the combination of P4 and TSA affected the stability of PRA and PRB. We first attempted to quantify PR expression in murine tissues but were unable to visualize the PRs using several different antibodies (table S3). Although we were unable to conduct these studies in mice, we were able to bridge the gap to humans using hTERT-HM$^{A/B}$ cells. These cells are a subline of a telomerase-immortalized myometrial cell line developed from uterine tissue from a premenopausal woman (*60*). hTERT-HM$^{A/B}$ cells have been modified to express PRA and PRB in response to doxycycline (DOX) and diacylhydrazine (DAH), respectively, allowing for control over PR expression to mimic that in the term myometrium (*29*, *61*). Figure 6A shows PRA and PRB induction in hTERT-HM$^{A/B}$ cells using DOX and DAH. After 24-hour incubation with either P4 or TSA alone, there was no change in the PRA:PRB ratio, as compared to the control cells (Ctrl), whereas the combination of P4/TSA significantly decreased the PRA:PRB ratio in the hTERT-HM$^{A/B}$

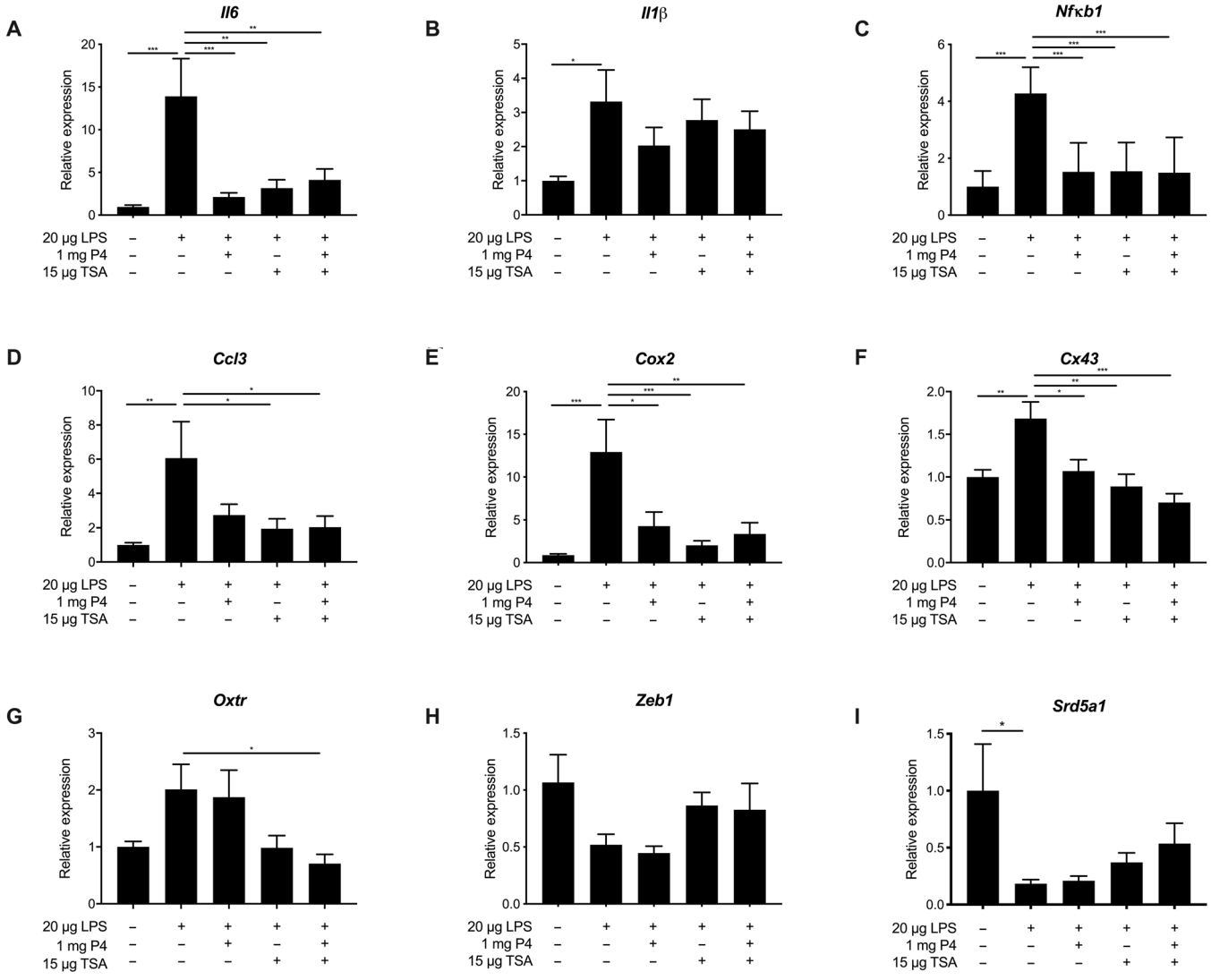

Fig. 5. Myometrial gene expression in different treatment groups. Relative gene expression for (**A**) *Il6*, (**B**) *Il1*β, (**C**) *Nfκb1*, (**D**) *Ccl3*, (**E**) *Cox2*, (**F**) *Cx43*, (**G**) *Oxtr*, (**H**) *Zeb1*, and (**I**) *Srd5a1* in myometrial tissue from dams receiving DDI of saline or DDI of LPS with no treatment, vaginal P4 NS (1 mg), TSA NS (15 μg), or P4/TSA NS (1 mg/15 μg). Gene expression was analyzed using the ΔΔCT method, using *Rplp0* as the housekeeping gene. Results are presented as expression relative to that in the saline sham–treated group. Data are shown as means ± SEM ($n \geq 8$). *$P < 0.05$, **$P < 0.01$, and ***$P < 0.001$

cells ($P = 0.032$) (Fig. 6B). A lower PRA:PRB ratio promotes an anti-inflammatory action of P4 (*29*). The results here support the hypothesis that the combination of P4/TSA modulates PR expression in a manner that supports the anti-inflammatory action of P4.

P4/TSA concentrations in mouse myometrial tissue after vaginal dosing in vivo suppress contractility in human myometrial cells in vitro

We next sought to characterize how the P4/TSA drug combination affects contractility in human myometrial cells. Drug concentration ranges tested were based on peak drug concentrations measured in mouse myometrial tissue after vaginal drug dosing in the pharmacokinetic experiments shown in Fig. 4. We first analyzed cell viability upon incubation with P4 and TSA alone and in combination. P4 was toxic to cells at the higher concentrations tested (20 and 40 μM), although the cell viability was increased when coincubated with 0.5 μM TSA (fig. S10). The PHM1-41 cells were then embedded in collagen to analyze how various drug concentrations affected contractility. Figure 6C shows the percentage of contraction at 96 hours. A black square represents 100% contraction, and a white square represents 0% contraction. Wells treated with a combination of 20 μM P4 with 0.5 μM TSA showed the least amount of contraction, decreasing in surface area by an average of 5.4 ± 4.1%. Conversely, cells treated with 20 μM P4 alone contracted 37.7 ± 13.8% ($P = 0.002$ compared to P4/TSA), and cells treated with 0.5 μM TSA alone contracted 46.8 ± 21.4% ($P = 0.001$ compared to P4/TSA), indicating that the combination of P4/TSA was the most effective at suppressing contractility.

Vaginal treatment with another HDAC inhibitor is effective for prevention of inflammation-induced PTB

We then tested the generalizability of our observations with another broad-spectrum HDAC inhibitor, suberoylanilide hydroxamic acid

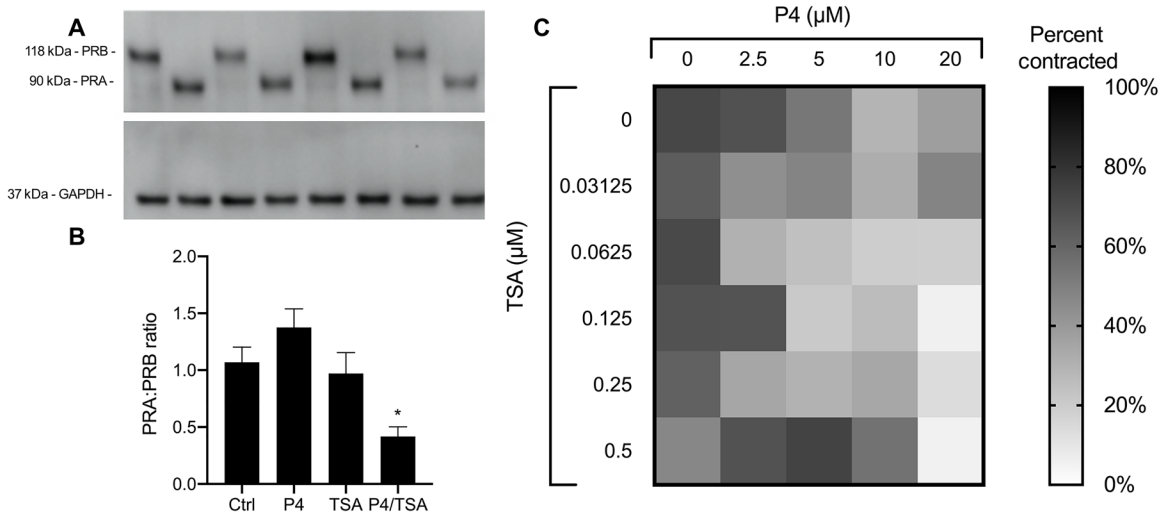

Fig. 6. Cell studies to investigate PRA:PRB ratio and myometrial contractility. (**A**) Representative Western blot showing stability of induced PRA and PRB in hTERT-HM$^{A/B}$ cells cultured in the presence of P4, TSA, or P4/TSA for 24 hours. GAPDH, glyceraldehyde-3-phosphate dehydrogenase. (**B**) Quantification of PRA:PRB ratio. Data are shown as means ± SEM ($n = 3$). *$P < 0.05$ compared to untreated cells (Ctrl). (**C**) Contraction of PHM1-41 cells in a collagen gel after incubation with P4 and TSA at various concentrations. The percentage of contraction was calculated at 96 hours based on gel area relative to the negative control (empty well, 0% contraction). Data are presented as the means ($n \geq 6$).

(SAHA) (*62*, *63*). Similar to TSA, SAHA is hydrophobic, facilitating NS formulation via wet milling (*64*). On the basis of the similarity in the structures of SAHA and TSA, we were able to formulate SAHA NS at a concentration of 1.5 mg/ml in a 1.5-ml tube stabilized by 4% F127 (Table 1). In contrast to the P4 NS, the SAHA NS rapidly reached a plateau in size and PDI within the first 2 hours of milling (Fig. 7A). As shown in Fig. 7B, vaginal administration of SAHA (15 μg) significantly reduced the PTB rate to 42% (7 of 12) as compared to 90% in the LPS control group (18 of 20; $P = 0.001$). Vaginal administration of 1 mg of P4/SAHA NS (1 mg/15 μg) also significantly reduced the PTB rate to 50% (6 of 12) as compared to the LPS control group ($P = 0.0013$). The SAHA NS treatment resulted in higher and less variable pup viability in live litters than P4/SAHA NS treatment (Fig. 7C). Individual term litter viability is shown in fig. S4. The female pups in the P4/SAHA NS group showed a significant 1.3-fold decrease in brain weight as a percentage of body weight as compared to the saline sham–treated group ($P = 0.027$) (Fig. 7D). When performing behavioral analyses for the SAHA and P4/SAHA groups, we tested on later days (PND 8 and 15) because animals in the previous study (Fig. 3, F to K) demonstrated high rates of failure on PND 5 (table S2). Testing on PNDs 8 and 15 has been used in other fields to gauge development (*65*). When comparing the SAHA NS and P4/SAHA NS groups to pups from dams receiving saline sham surgery, there were no differences for cliff aversion (Fig. 7E). No differences were observed in negative geotaxis (Fig. 7F) or in surface righting (Fig. 7G) on PND 8 or 15. On PND 8, the P4/SAHA NS group spent fivefold more time in the center than the saline sham group ($P = 0.017$) (Fig. 7H). This could indicate decreased motor skills, increased anxiety, or decreased cognition (*66*–*68*).There were no differences in distance traveled (Fig. 7I) or average velocity (Fig. 7J) in the open field for the P4/SAHA NS group, as compared to the saline group.

DISCUSSION

Although our medical technologies for saving preterm infants have markedly improved over the past several decades (*69*), the worldwide rates of PTB have remained relatively steady (*4*). In the United States, PTBs still account for ~10% of pregnancies, a rate higher than in most other developed countries (*70*). Intrauterine inflammation is known to cause nearly 30% of all PTBs and is associated with fetal neurological deficits (*4*). P4 and its synthetic analogs have been used clinically with varied success (*5*, *16*, *20*, *32*, *37*). In 1962, a small clinical trial revealed that P4 therapy did not prevent infection-mediated parturition but was able to prevent parturition caused by P4 withdrawal (*71*). More recently, the only FDA-approved therapy for PTB prophylaxis, an intramuscular injection of 17-OHPC (Makena), failed a confirmatory trial, resulting in the CDER's recommendation to withdraw Makena's FDA approval (*6*–*9*). Vaginal P4 formulations have also been used off-label as prophylactic options for PTB; however, inconsistent efficacies across several clinical trials have precluded FDA approval for the prevention of PTB (*10*, *72*, *73*).

Vaginal administration of therapeutics is preferred for targeting the female reproductive tract (*12*, *74*). Systemically administered drugs are diluted because they are transported throughout the more than 150,000 kilometers of vasculature in the adult human body before reaching their intended site of action (*75*). It was previously shown that systemic administration of P4 led to 10-fold less accumulation in the endometrium compared to vaginal P4 administration, despite the fact that the plasma concentrations after systemic administration were sevenfold higher than concentrations resulting from vaginal P4 administration (*11*). As a vaginally administered drug is absorbed, it is circulated directly to the uterine tissues by the vasculature surrounding the female reproductive tract, termed the uterine first-pass effect (*11*). However, the CVM barrier, which serves to protect underlying tissue and, in the case of pregnancy, the developing fetus, limits the effectiveness of vaginal drug absorption. To overcome the CVM barrier, we have formulated hydrophobic drugs, such as P4, for vaginal administration as a mucoinert NS, which leads to increased local delivery to reproductive tract tissues compared to Crinone gel (*15*). With Pluronic F127 as the stabilizing agent, we developed mucoinert NS formulations for various drug loadings of P4, as well as for HDAC

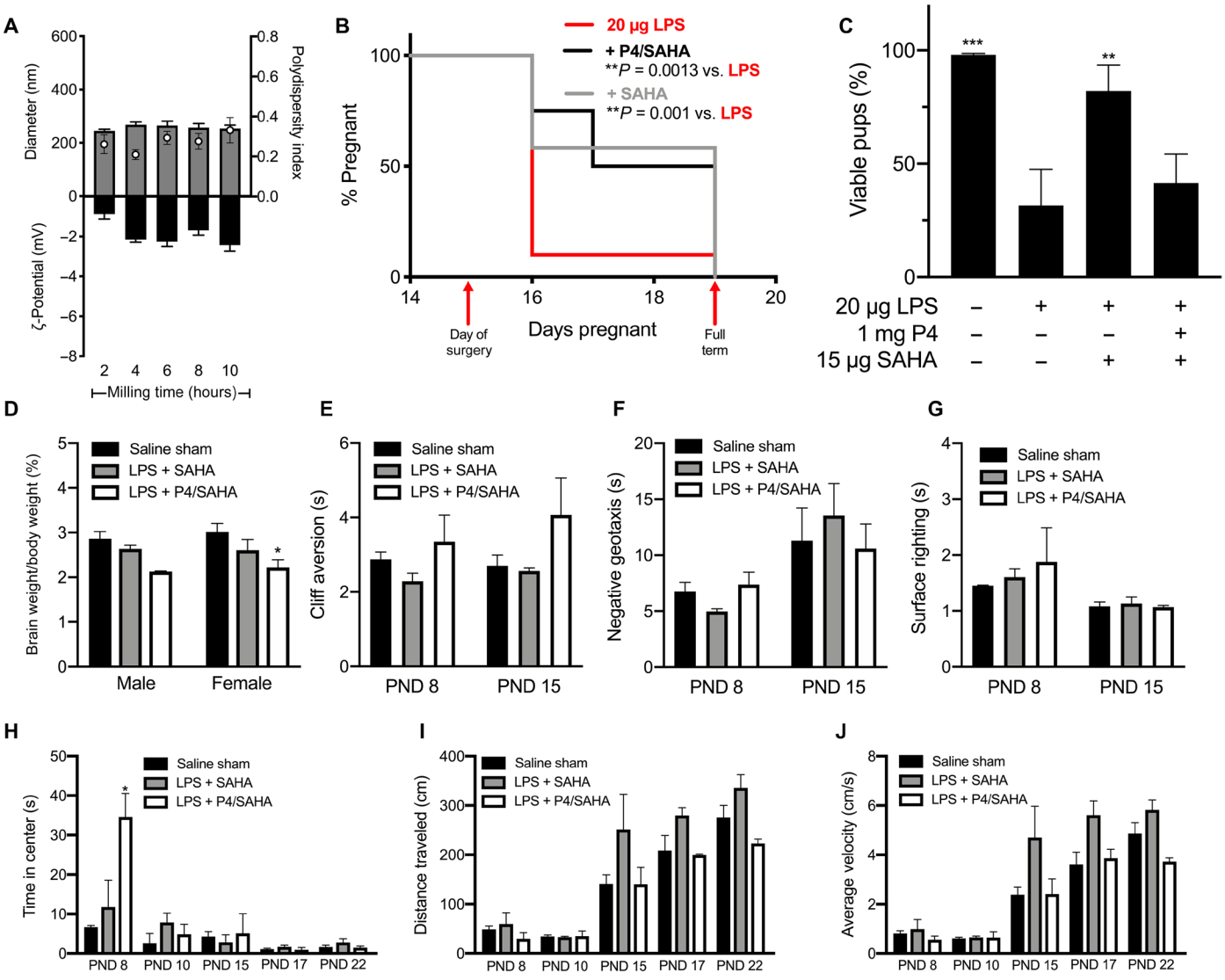

Fig. 7. PTB prevention and behavioral analyses for P4/SAHA treatments. (**A**) Diameter (gray bars), PDI (white dots), and ζ-potential (black bars) of SAHA NS (1.5 mg/ml) over 10 hours of nanomilling. Data are represented as means ± SEM ($n \geq 3$). (**B**) Pregnancy survival curves showing the percentage of animals remaining pregnant after DDI of 20 µg of LPS on E15. Daily vaginal administration of various doses of SAHA NS (15 µg, $n = 12$) or P4/SAHA (1 mg/15 µg, $n = 12$) provided a significant reduction in PTB rates compared to LPS alone ($n = 20$) (**$P < 0.005$, Mantel-Cox test). (**C**) For term litters, the percentage of pups born live compared to viable pups counted on E15. **$P < 0.001$ and ***$P < 0.0001$ compared to LPS. Data are presented as means ± SEM ($n \geq 12$ litters). (**D**) Pup brain weight as a percentage of body weight for pups from the saline sham–treated, 20 µg of LPS + SAHA (15 µg), or LPS + P4/SAHA (1 mg/15 µg) group. *$P = 0.027$. (**E** to **J**) Behavioral tests for pups in the saline sham–treated, 20 µg of LPS + SAHA (15 µg), or LPS + P4/SAHA (1 mg/15 µg) group: (E) cliff aversion, (F) negative geotaxis, (G) surface righting, (H) time in center for open field (*$P = 0.02$), (I) distance traveled in open field, and (J) average velocity in open field. Failures were not included in data analysis. Data are presented as means ± SEM ($n \geq 3$ litters).

inhibitors TSA and SAHA. Pharmacokinetic studies showed that both P4 and TSA reach local tissues (cervix and myometrium) with sustained exposure for up to 8 hours. In addition, similar to our prior study (*15*), we observed double peaks in P4 concentration, reflecting recirculation from the uterus (*76*–*78*). When dosed vaginally, the combination of P4/TSA NS prevented intrauterine LPS-induced PTB. However, systemic administration of the same P4/TSA dose had no effect. This could be due to the lower pharmacodynamic availability of the drug in the uterus when delivered systemically.

In mouse models of inflammation-induced PTB, progestins have been tested to evaluate their ability to decrease markers of inflammation, alleviate fetal brain injury, and prevent PTB (*32*–*34*, *38*, *79*, *80*). Throughout these studies, different standards were used to evaluate potential efficacy of therapeutics. Some studies evaluated for delay of PTB over the following 18 to 24 hours after induction, whereas others reported a difference in timing to delivery of nonviable pups as compared to the positive control (*81*). Here, we defined successful prevention of PTB as delivery of live pups at term. In addition, our model of PTB involved counting the number of live pups in utero on the day of surgery, allowing us to calculate the percentage of viable pups born on E19 to E20 (*39*). We have shown that 17-OHPC and P4 alone are not capable of preventing

inflammation-induced PTB. However, when combining vaginal P4 with an HDAC inhibitor (TSA or SAHA), we were able to prevent PTB, resulting in live pups, and increase the average pup viability in litters born at term. Furthermore, pups from the P4/TSA NS group performed similarly to their saline sham counterparts in neurological development tests. This is particularly encouraging because exposure to intrauterine inflammation is associated with fetal neurological deficits (*18*, *36*). By these criteria, we have demonstrated that the combination of vaginal P4/TSA is effective in preventing intrauterine inflammation–induced PTB, resulting in live, neurotypical offspring in a preclinical animal model.

The PR occurs in two predominant isoforms, PRA and PRB. P4 shows differential action based on receptor expression (*27*, *82*). Tan *et al.* (*29*) demonstrated that PRB promotes the anti-inflammatory effect of P4, whereas PRA inhibits the anti-inflammatory action. As gestation progresses, the ratio of PRA:PRB increases in human myometrium due to the repression of PRA on the transcriptional activity of PRB (*29*). The increased ratio of PRA:PRB decreases the responsiveness of myometrial cells to P4, allowing the proinflammatory event of labor to occur (*30*). In mice, PRB expression is decreased at the onset of inflammation-induced PTB (*37*). In this study, we investigated changes in myometrial cells based on our previous study, where we observed the DDI of LPS having the most impact on myometrial contractions (*39*). To bridge the gap from mice to humans, we used hTERT-HM$^{A/B}$ cells, which have been used to characterize the role of PRA:PRB ratio in the context of human labor (*29*, *61*). Using hTERT-HM$^{A/B}$ cells, we showed that the combination of P4 and TSA decreased the PRA:PRB ratio in vitro. In vivo, we observed that all treatment groups (P4, TSA, and P4/TSA) showed anti-inflammatory effects in myometrial tissue. Although vaginal P4 alone was unable to prevent inflammation-induced PTB in our model, we observed that treatment with vaginal P4 decreased the expression of *Il6*, *Nfκb1*, *Ccl3*, *Cox2*, and *Cx43*. Similarly, others have described that treatment with progestins decreased the expression of several proinflammatory markers in both myometrial and cervical tissues, although this did not result in delivery of live pups (*33*, *34*, *37*). Here, the combination of vaginal P4/TSA led to a greater reduction of *Ccl3*, *Cox2*, *Cx43*, and *Oxtr* expression in the myometrium than P4 alone and resulted in the delivery of live pups at term.

PRA and PRB have also been shown to play opposing roles in the onset of uterine contractions (*29*). PRB promotes uterine quiescence by decreasing *Cx43* expression, whereas PRA promotes *Cx43* expression and gap junction formation, thereby facilitating contractions (*61*). Using PHM1-41 cells in vitro, we observed that the peak concentration of P4/TSA quantified in murine tissue during pharmacokinetic studies was the most effective in preventing human myometrial cell contractility in vitro. In vivo, we observed that P4/TSA down-regulated *Cx43* expression, as compared to the LPS group. Furthermore, only the P4/TSA group was able to down-regulate *Oxtr* expression. We hypothesize that TSA promotes PRB expression, which, in turn, promotes uterine quiescence. Taking into account our results from previous studies (*29*, *30*, *37*, *61*, *83*), it is possible that our model of inflammation-induced PTB alters the PR ratio in vivo, resulting in a more PRA-dominated state and explaining why P4 alone is unable to prevent PTB.

The role of HDAC inhibitors in parturition has been studied previously (*40*–*43*, *84*). Condon and co-workers (*43*) found that a decrease in histone acetylation in human myometrium at term corresponded to an increase in histone acetyltransferase activity that led to loss of the anti-inflammatory action of P4 and, thus, initiation of labor. They then demonstrated that systemic administration of TSA to pregnant dams was able to prolong gestation (*43*). Lindstrom *et al.* (*85*) described the time-dependent effects of HDAC inhibitors in vitro. Using both TSA and SAHA, they showed that *Nfκb1* activity was decreased by HDAC inhibitor treatment, resulting in an immunosuppressive response (*85*). In human placental explants, Munro *et al.* (*40*) showed that TSA decreased tumor necrosis factor–α (*Tnfα*) and *Il10* expression, as compared to an LPS challenge. In human myometrial tissues ex vivo, Ilicic *et al.* (*47*) showed that TSA is capable of promoting and maintaining a low PRA:PRB ratio. We hypothesize that administering an HDAC inhibitor in combination with P4 supports the expression of PRB, promoting the anti-inflammatory action of P4 to prevent the labor process. The results described herein support the growing evidence that epigenetic changes in the PRA:PRB ratio play a role in mediating the timing of parturition.

We have previously described that preclinical model adaptation can be key to studying drug treatment efficacy for preventing PTB in vivo (*15*). Similarly, here, we used our recently described adapted model of intrauterine inflammation that uses two distal injections of LPS instead of SPI (*39*). DDI leads to uniform exposure of LPS in the uterine horns, resulting in increased PTB rates with lower doses of LPS (*39*). Using this murine model, we were able to test therapies for prevention of inflammation-induced PTB that resulted in the birth of live offspring. One potential limitation is that the HDAC inhibitors used in these studies have broad-spectrum epigenetic activity and that there is the potential for unwanted off-target side effects, especially in the context of pregnancy and fetal development (*86*–*88*). Nonetheless, we have demonstrated the importance of effective drug delivery in understanding drug action. Both the mechanistic implications and the methodology for studying the effects of the drug candidates investigated here should have impact on the field.

We have not yet investigated the pathways by which HDAC inhibitors contribute to the prevention of inflammation-induced PTB. Detailed mechanistic studies, such as investigation of protein acetylation, would better elucidate the role of HDAC inhibitors in preventing PTB. In addition, it has previously been demonstrated that different HDAC inhibitors have different biodistribution profiles and rates of metabolism after oral and intravenous dosing in mice (*64*). It is possible that SAHA without P4 supplementation was more effective than TSA alone in preventing PTB because of improved delivery in the reproductive tract after vaginal administration. PK studies would be helpful in this regard. Further, we were unable to characterize the impact of treatment on cervical remodeling because we observed no differences in expression of select genes previously shown to be implicated in cervical remodeling (*58*). Further investigation should be performed to characterize the role of cervical remodeling in the DDI model of PTB, as well as how HDAC inhibitors may affect gene expression in the cervix. Additional studies should be performed to explore toxicity and teratogenic profiles of HDAC inhibitors, as well as to identify the ratio of P4:HDAC inhibitor that shows the best efficacy of PTB prevention. The potential for single-agent therapy that does not require additional exogenous P4 is also of high interest. Because PTB prevention with TSA alone was not statistically different from that observed with P4/TSA, it may be possible to find an optimal TSA dose that would be

effective without P4, similar to what was observed with SAHA. In regard to fetal development, future experiments should investigate sex-related differences in development. It will also be important to investigate mechanisms that lead to preservation of neurological development, including the decrease in endotoxin content we observed in amniotic fluid and beyond.

There is a paucity of effective treatments for the prevention of PTB. Clinically used therapies have shown a lack of prevention in recent trials (*5*, *6*, *89*). The results presented here contribute to the identification of therapeutic pathways for the prevention of inflammation-induced PTB. Better understanding of these pathways has the potential to save lives from the effects of prematurity. Moving forward, the techniques described here could be used to identify additional drug candidates with more targeted action that may be more appropriate for use during pregnancy. Further, effective drug delivery to the cervix and uterus can facilitate drug discovery and development for a wide range of conditions and diseases, including uterine fibroids, reproductive tract cancers, infertility, and infections, as well as the development of additional nonsystemic contraceptives.

MATERIALS AND METHODS

Study design

Here, we tested clinically used formulations, as well as engineered nanoformulations of P4, TSA, and SAHA for the prevention of PTB in an established murine model. We analyzed maternal responses with PK and reverse transcription quantitative polymerase chain reaction (RT-qPCR) experiments and fetal outcomes using neurobehavioral tests. We further analyzed drug action in human cells using Western blot and contraction assays. RT-qPCR experiments, PK studies, and behavioral analyses were performed in a blinded manner. Pregnancy "survival" studies, NS formulations, and cell studies were not blinded. In survival studies, dams were randomly assigned to treatment groups.

Animals

Timed pregnant 6- to 8-week-old CD-1 dams were ordered from Charles River Laboratories and arrived on E13. PTB induction was performed on E15. Dams were housed in a normal light cycle room (dark hours, 8 p.m. to 8 a.m.). All procedures were approved by the Johns Hopkins University Animal Care and Use Committee.

Intrauterine LPS model of inflammation-induced PTB

An established model of DDI of LPS was used to induce inflammation-induced PTB (*39*). Briefly, two intrauterine, extra-amniotic injections of 50 μl of sterile normal saline (sham) or LPS (Sigma-Aldrich; 055:B5 *Escherichia coli* purified via phenol extraction, lot #28M4094V) dissolved in normal saline were given between the two pups most distal from the cervix in each uterine horn (total LPS dose, 5 to 20 μg). The total number of pups on E15 was noted. After surgery, dams were checked at 2-hour intervals for signs of PTB (vaginal bleeding, bloody bedding, and presence of pups). After the first 12 hours, dams were checked every 12 hours. PTB usually occurred within 8 to 10 hours in the LPS induction group. PTB was defined as delivery before E19. Litter resorption was counted as PTB. Pups delivered at term were counted, and the percentage of viable fetuses was calculated on the basis of the number of live pups counted at the time of surgery.

NS formulation and characterization

In order for vaginal drug delivery to be effective, formulations must be engineered to bypass the mucus barrier (*12*, *14*, *15*). We have previously shown that to penetrate through the sticky mesh of mucin proteins in CVM, nanoparticles should be less than 500 nm in size and coated with mucoinert polymers to prevent adhesive interactions (*12*, *15*). More recently, we have demonstrated that the pore size is decreased in CVM samples from pregnant women, likely due to increasing endogenous amounts of P4 throughout gestation (*15*). Our previous studies have shown that Pluronic F127 coating leads to increased particle mobility in mucus ex vivo (*14*, *15*), which directly correlates to enhanced vaginal particle distribution and drug delivery in vivo (*12*). Further, formulating hydrophobic drugs as NS increases the surface area to volume ratio for improved drug dissolution and local tissue absorption (*14*, *90*). In addition, by delivering particles hypotonically, the osmotic gradient promotes the uniform distribution of particles throughout the cervicovaginal tract (*13*). Using these criteria, we formulated progesterone (P4, P8783-5G, Sigma-Aldrich), TSA (Bio-Techne), and SAHA (catalog 10009929, Cayman Chemical) into mucoinert NS using a wet milling approach, as previously described (*15*). Briefly, drugs were placed in an Eppendorf tube with metal beads (Next Advance), and a bead-based tissue homogenizer (TissueLyser LT, QIAGEN) was used to reduce particle size. Pluronic F127 (BASF) dissolved in water (1 to 6%, w/v) was used to stabilize the NS. Wet milling was performed for 10 hours at 4°C. To determine the final formulation parameters for the NS, the tube size, bead type, bead mass, and polymer concentration were varied (table S1). A Malvern Zetasizer Nano ZS (173° scattering angle) was used to analyze particle size, PDI, and surface charge (ζ-potential) of all NS. Final formulations were chosen on the basis of having a size that could fit through the pore sizes of CVM (<~380 nm), a PDI less than 0.25 to indicate relative uniformity in particle size, and a net-neutral ζ-potential reflecting sufficient surface shielding to avoid adhesive interactions with mucin proteins (*12*, *14*). The final formulations used in this study can be found in Table 1, where each value is an average of $n = 3$ particle batches. In all cases, particle size was confirmed before use to ensure uniformity between batches.

Administration of therapeutics to prevent inflammation-induced PTB

Treatments were dosed daily, with the first dose after surgery on E15 and the last dose on E18. Treatment ceased if dams delivered prematurely. 17-OHPC (Makena) was administered intraperitoneally at a dose of 80 μg in 100 μl of castor oil with benzyl benzoate and benzyl alcohol, as previously described (*91*). We used a dose of 80 μg of 17-OHPC (Makena), converting from the human dose of 250 mg (*92*). P4 was administered vaginally as either Crinone gel or as an NS. Dams that received P4 as vaginal gel received 100 μl of 8% Crinone (8 mg of P4) using a Wiretrol (Drummond Scientific) due to the high viscosity. P4 NS were administered using a standard pipette at doses of 100 μg (20 μl, 5 mg/ml, $n = 5$), 500 μg (20 μl, 25 mg/ml, $n = 8$), 1 mg (20 μl, 50 mg/ml, $n = 20$), or 5 mg (20 μl, 250 mg/ml, $n = 5$). For P4 PT studies, dams received doses of 8 mg of P4 NS on E13 and E14, with surgery occurring on E15, followed by the standard dosing schedule. TSA NS was administered vaginally at a dose of 15 μg (10 μl, 1.5 mg/ml, $n = 20$). TSA NS (15 μg) was coadministered vaginally with P4 NS at doses of 100 μg ($n = 7$), 500 μg ($n = 19$), 1 mg ($n = 20$), or 5 mg ($n = 10$) for a total volume of 30 μl

($n \geq 7$). The combination of P4 (1 mg) and TSA (15 μg) was also administered intraperitoneally in 200 μl of sterile dimethyl sulfoxide (DMSO) ($n = 8$). SAHA NS was administered vaginally at a dose of 15 μg (10 μl, 1.5 mg/ml, $n = 12$). P4 NS (1 mg) and SAHA NS (15 μg) were coadministered vaginally for a total volume of 30 μl ($n = 12$). Vehicle control studies were performed by dosing 30 μl of 4% F127 ($n = 6$). PTB was defined as delivery before E19.

Behavioral analysis

Pups were assessed for developmental milestones, as previously described (*36*, *66*). Labyrinthine reflex, strength, coordination (cliff aversion and surface righting), and motor skills (negative geotaxis test) were assessed on PNDs 5 and 9 (P4/TSA, $n = 6$ litters) or PNDs 8 and 15 (SAHA, $n = 6$ litters; P4/SAHA, $n = 4$ litters). Cognition and motor skills were assessed with an open field test on PNDs 9, 13, 15, 17, and 22 (P4/TSA) or PNDs 8, 10, 15, 17, and 22 (SAHA and P4/SAHA). For both cliff aversion and negative geotaxis tests, pups were filmed performing the task three times. Videos were analyzed in a blinded manner, and the time to complete each task was averaged for each pup. In the open field test, pups were placed in the center of a 10-cm circle in the center of a 30 cm by 60 cm box. They were filmed for 1 min, and their time in the center, distance traveled, and average velocity were calculated using Noldus EthoVision XT. On PND 22, pups were euthanized, and brains were collected to determine the brain weight as a percentage of body weight. Each testing scheme included a minimum of $n = 3$ saline sham–treated litters.

Pharmacokinetics

Healthy pregnant dams ($n = 3$ per group, per time point) were dosed vaginally with P4 NS (1 mg) or P4/TSA NS (1 mg/15 μg). Plasma, cervix, proximal myometrium, and distal myometrium were collected at 1, 2, 3, 4, 6, 8, and 12 hours after drug administration. Dams were anesthetized under constant 2% isoflurane, and blood was collected via cardiac puncture. The blood was centrifuged for 10 min at 1300 relative centrifugal force (rcf) in EDTA-coated tubes to separate plasma. Upper (distal to the cervix) and lower (proximal to the cervix) myometrial tissue was collected, and the decidua was removed using a disposable razor blade and gently scraped the tissue. The cervix was isolated under a dissecting microscope, taking care to remove any excess vaginal or myometrial tissue. P4 concentration was measured in cervical and myometrial tissue as previously described (*15*, *39*).

TSA was quantified using a standard curve and quality control samples prepared in charcoal-stripped (2×) mouse K2 EDTA plasma (BioIVT). Tissue samples were homogenized in 200 or 400 μl of blank charcoal-stripped mouse plasma using ULTRA-TURRAX T25 homogenizer (IKA) before extraction. TSA was extracted from 50 μl of plasma or tissue homogenates with 0.5 ml of acetonitrile/*n*-butyl chloride (1:4, v/v) containing 40 ng/ml of the internal standard, progesterone-d9 (Toronto Research Chemicals). After centrifugation, the top layer was then transferred to a clean glass tube and dried in a 40°C water bath under a stream of nitrogen gas. The samples were reconstituted with 100 μl of water/acetonitrile (50:50, v/v) and then transferred into autosampler vials for liquid chromatography–tandem mass spectrometry analysis. Separation was achieved with an Agilent ZORBAX XDB, C18 (4.6 mm by 50 mm, 5 μm) column at room temperature with a gradient of water (mobile phase A), and acetonitrile (mobile phase B) containing 0.1% (v/v) formic acid with a flow rate of 0.7 ml/min. The gradient started with mobile phase B held at 50% for 0.5 min and increased to 100% over 0.5 min; 100% mobile phase B was held for 1.5 min, then returned back to 50% mobile phase B, and allowed to equilibrate for 0.5 min. Total run time was 3 min. The column effluent was monitored using a Sciex triple quadrupole 5500 mass spectrometric detector (Sciex) using electrospray ionization operating in positive mode. The spectrometer was programmed to monitor the following multiple reaction monitoring (MRM) transitions: 303.0 → 148.0 for TSA and 324.3 → 100.0 for the internal standard, progesterone-d9. Calibration curves for TSA were computed using the area ratio peak of the analysis to the internal standard using a quadratic equation with a 1/×2 weighting function over the range of 0.2 to 200 ng/ml with dilutions of up to 1:1000 (v/v).

TSA is quickly metabolized. Others have demonstrated that the biotransformation of TSA occurs rapidly when dosed intraperitoneally to dams (*50*) and that rapid biotransformation of TSA occurs similarly in both rat and human hepatocytes (*93*). Metabolites for TSA were also monitored and quantitated on the basis of the calibration curve for TSA because an authentic reference standard was not available at the time. Mass spectrometer transitions were based on data published by Sanderson *et al.* (*50*). Phoenix 32 WinNonlin software was used to calculate the AUC.

Myometrial and cervical gene expression

Intrauterine saline or LPS injections were performed as described above. For dams receiving LPS injections, a single vaginal treatment with saline, P4 NS (1 mg), TSA NS (15 μg), or P4/TSA NS (1 mg/15 μg) was given immediately after surgery ($n \geq 8$ dams per group). After 8 hours, myometrial and cervical tissues were collected from each dam. Myometrial tissue was collected from both the left and the right lower uterine horns and combined for each dam. The decidua was removed using a disposable razor blade to gently scrape the tissue. Cervical tissue was isolated using a dissection microscope to completely remove the vaginal and uterine tissue. Samples were frozen with liquid nitrogen and stored at −80°C until processing. In addition, amniotic fluid was collected by pooling fluid from three to five amniotic sacs per dam to achieve a total volume of 1 ml. Samples were frozen with liquid nitrogen and stored at −80°C until processing, as described below. RNA was isolated as previously described (*39*). Briefly, thawed tissues were homogenized in 1 ml of TRIzol (catalog 15596026, Thermo Fisher Scientific) using an IKA T10 probe homogenizer with an S10N-10G-ST dispersion element. Samples were centrifuged, and the supernatant was processed using the RNeasy Mini Kit (QIAGEN). RNA concentration was measured, and complementary DNA (cDNA) was produced using a high-capacity cDNA reverse transcription kit (Applied Biosystems, catalog 4368813). PCRs were run in triplicate. Primer sequences can be found in table S4. The $\Delta\Delta C_T$ method was used to analyze gene expression, normalized to acidic ribosomal phosphoprotein P0 (*Rplp0*).

Endotoxin assay

Amniotic fluid samples were thawed on ice. As previously reported, a ToxinSensor chromogenic LAL endotoxin assay kit (GenScript #L00350) was used to analyze endotoxin concentrations (*39*). Samples were each run in triplicate.

hTERT-HM$^{A/B}$ human myometrial cells

hTERT-HM$^{A/B}$ cells were used to study the differential effects of P4 and TSA on PRA and PRB. As previously described, hTERT-HM$^{A/B}$

cells are used to control PR isoform expression, which allows for modeling the changing PR content in the human myometrium over the course of gestation (*61*). Cells were cultured in 1:1 Dulbecco's modified Eagle's medium (DMEM):Ham's F12 supplemented with 5% charcoal-stripped fetal bovine serum (FBS), 0.5% penicillin/streptomycin (P/S), 2 mM glutamine, geneticin (100 μg/ml), hygromycin B (1 μg/ml), and blasticidin (5 μg/ml) (*61*). Cells were incubated with DOX (100 ng/ml) and 500 nM DAH for 48 hours to induce PRA and PRB, respectively. After induction of PRA and PRB, cells were incubated with drug in DMSO (final concentration in medium, <1%) for 24 hours. On the basis of previous studies, we used P4 at a concentration of 100 nM (*61*). To maintain the drug ratio observed in mouse myometrium tissue in vivo, TSA was used at a concentration of 2.5 nM.

Protein extraction and Western blot

In testing several antibodies, we were unable to visualize murine PR in Western immunoblots (*94*). hTERT-HM$^{A/B}$ cell lysates were collected in T-PER Tissue Protein Extraction Reagent (Thermo Fisher Scientific, catalog 78510) supplemented with protease inhibitor following the supplier's instructions (cOmplete, Mini, EDTA-free Protease Inhibitor Cocktail, Roche, 11836170001). Protein was extracted by vortexing samples, followed by centrifugation at 15,000 rpm for 10 min at 4°C. Protein concentration was determined using Pierce BCA Protein Assay Kit (Thermo Fisher Scientific, catalog 23225). Equivalent amounts of protein were separated via SDS–polyacrylamide gel electrophoresis. Samples were transferred to a polyvinylidene difluoride membrane, which was subsequently blocked in 3% bovine serum albumin in tris-buffered saline with 0.1% Tween 20 (TBS-T) for 2 hours at room temperature. The membrane was then incubated in primary antibodies at 4°C overnight. The membrane was washed in TBS-T 3× for 5 min each and then incubated in peroxidase-conjugated anti-mouse immunoglobulin G (Jackson ImmunoResearch, catalog 715-035-150) at room temperature for 1 hour. Antibodies used in this study can be found in table S3. Proteins were detected using chemiluminescence reagent (Bio-Rad chemiluminescence) and imaged using the ChemiDoc Imaging System.

PHMI-41 human myometrial cells

PHMI-41 cells were obtained from the American Type Culture Collection. Cells were cultured in DMEM supplemented with 2 mM glutamine, 10% heat-inactivated FBS, and 1% P/S in a sterile 37°C incubator with 5% CO_2. Cells were passaged every 4 days using 0.05% trypsin-EDTA and collected the same way. Experiments were performed at 80 to 90% confluency. To assess cell viability after drug exposure, cells were seeded in 96-well plates in normal medium for 24 hours. Cells were treated with (i) 0.031, 0.063, 0.013, 0.25, or 0.5 μM TSA; (ii) 2.5, 5, 10, 20, or 40 μM P4; (iii) 0.5 μM TSA with either 2.5, 5, 10, 20, or 40 μM P4; and (iv) 20 μM P4 with either 0.031, 0.063, 0.013, 0.25, or 0.5 μM TSA. Drugs were solubilized in 1% DMSO. Control cells received no treatment. Each group contained a minimum of $n = 6$ wells. The Dojindo Cytotoxicity Assay Kit (Dojindo Molecular Technologies Inc., catalog CK04-01) was used according to the manufacturer's instructions. For the cell contractility assay, PHMI-41 cells were grown in collagen matrices, as previously described (*95*–*97*). Briefly, a type I collagen solution (Cultrex Rat Collagen I, R&D Systems, catalog 3440-100-01) was neutralized with 0.1 N of NaOH for a final collagen concentration of 1.5 mg/ml. Cells were added for a density of 150,000 cells per well. The suspension was allowed to gel in a 24-well plate for 2 hours at 37°C. Gels were carefully detached from wells, and fresh medium was added over the gel. Images were taken at 96 hours using ChemiDoc MP imaging system (Bio-Rad). Percentage of contraction was used by determining the gel area with ImageJ [National Institutes of Health (NIH)].

Statistical analysis

Results were analyzed in GraphPad Prism version 8.2.1. The Mantel-Cox test was used to compare pregnancy survival curves. For other comparisons involving two groups, a two-tailed Student's *t* test assuming unequal variance was used. For comparisons of three or more groups, one-way analysis of variance (ANOVA) was used followed by Tukey's multiple comparison test. Data are reported as means ± SEM. Experiments were performed multiple times to ensure reproducibility. A minimum of two negative controls (saline sham) and three positive controls (LPS induction) were included with each experiment. Efficacy experiments for vaginal NS (P4, TSA, P4/TSA, SAHA, and P4/SAHA) were performed a minimum of three times, with at least four dams in each group. Sample collection for both RT-qPCR and endotoxin quantification was performed twice to increase replicates.

SUPPLEMENTARY MATERIALS

stm.sciencemag.org/cgi/content/full/13/576/eabc6245/DC1

Fig. S1. PTB prevention for various doses of P4 with TSA.
Fig. S2. PTB prevention for F127 vehicle control.
Fig. S3. Histogram of litter sizes.
Fig. S4. Individual litter pup viability.
Fig. S5. Amniotic fluid endotoxin quantification.
Fig. S6. TSA metabolite PK.
Fig. S7. PK for 1 mg of P4 dosed alone.
Fig. S8. AUC for PK studies.
Fig. S9. Cervical gene expression.
Fig. S10. PHM1-41 cell viability.
Table S1. Formulation optimization for TSA NS.
Table S2. Pup behavior fail rates.
Table S3. Antibodies used in Western blotting.
Table S4. Primer sequences.

View/request a protocol for this paper from *Bio-protocol*.

REFERENCES AND NOTES

1. A. Parizek, M. Koucky, M. Duskova, Progesterone, inflammation and preterm labor. *J. Steroid Biochem. Mol. Biol.* **139**, 159–165 (2014).
2. B. M. Kuehn, Groups take aim at US preterm birth rate. *JAMA* **296**, 2907–2908 (2006).
3. H. Blencowe, S. Cousens, D. Chou, M. Oestergaard, L. Say, A. B. Moller, M. Kinney, J. Lawn; Born Too Soon Preterm Birth Action Group, Born too soon: The global epidemiology of 15 million preterm births. *Reprod. Health* **10** (suppl. 1), S2 (2013).
4. F. G. Cunningham, K. J. Leveno, S. L. Bloom, J. S. Dashe, B. L. Hoffman, B. M. Casey, C. Y. Spong, *Williams Obstetrics* (New York: McGraw-Hill, 2018), ed. 25.
5. S. C. Blackwell, C. Gyamfi-Bannerman, J. R. Biggio Jr., S. P. Chauhan, B. L. Hughes, J. M. Louis, T. A. Manuck, H. S. Miller, A. F. Das, G. R. Saade, P. Nielsen, J. Baker, O. M. Yuzko, G. I. Reznichenko, N. Y. Reznichenko, O. Pekarev, N. Tatarova, J. Gudeman, R. Birch, M. J. Jozwiakowski, M. Duncan, L. Williams, J. Krop, 17-OHPC to prevent recurrent preterm birth in singleton gestations (PROLONG Study): A multicenter, international, randomized double-blind trial. *Am. J. Perinatol.* **37**, 127–136 (2019).
6. R. Rubin, Confirmatory trial for drug to prevent preterm birth finds no benefit, so why is it still prescribed? *JAMA* **323**, 1229–1232 (2020).
7. E. N. Michael House, Progesterone supplementation does not PROLONG pregnancy in women at risk for preterm birth: What do we do now? *MDedge ObGyn* **31**, 36–38 (2019).
8. J. Pauli, Results from the PROLONG trial may shake up treatment options for recurrent preterm birth. *MDedge ObGyn* **32**, 15–28 (2020).

9. FDA CDER, qDER proposes withdrawal of approval for Makena," 5 October 2020; www.fda.gov/drugs/drug-safety-and-availability/cder-proposes-withdrawal-approval-makena?utm_medium=email&utm_source=govdelivery.
10. E. Yanushpolsky, S. Hurwitz, L. Greenberg, C. Racowsky, M. Hornstein, Crinone vaginal gel is equally effective and better tolerated than intramuscular progesterone for luteal phase support in in vitro fertilization-embryo transfer cycles: A prospective randomized study. *Fertil. Steril.* **94**, 2596–2599 (2010).
11. D. De Ziegler, C. Bulletti, B. De Monstier, A. S. Jääskeläinen, The first uterine pass effect. *Ann. N. Y. Acad. Sci.* **828**, 291–299 (1997).
12. L. M. Ensign, B. C. Tang, Y.-Y. Wang, T. A. Tse, T. Hoen, R. Cone, J. Hanes, Mucus-penetrating nanoparticles for vaginal drug delivery protect against herpes simplex virus. *Sci. Transl. Med.* **4**, 138ra179 (2012).
13. L. M. Ensign, T. E. Hoen, K. Maisel, R. A. Cone, J. S. Hanes, Enhanced vaginal drug delivery through the use of hypotonic formulations that induce fluid uptake. *Biomaterials* **34**, 6922–6929 (2013).
14. T. Yu, J. Chisholm, W. J. Choi, A. Anonuevo, S. Pulicare, W. Zhong, M. Chen, C. Fridley, S. K. Lai, L. M. Ensign, J. S. Suk, J. Hanes, Mucus-penetrating nanosuspensions for enhanced delivery of poorly soluble drugs to mucosal surfaces. *Adv. Healthc. Mater.* **5**, 2745–2750 (2016).
15. T. Hoang, H. Zierden, A. Date, J. Ortiz, S. Gumber, N. Anders, P. He, J. Segars, J. Hanes, M. Mahendroo, L. M. Ensign, Development of a mucoinert progesterone nanosuspension for safer and more effective prevention of preterm birth. *J. Control. Release* **295**, 74–86 (2019).
16. R. M. Silver, F. G. Cunningham, Deus ex Makena? *Obstet. Gynecol.* **117**, 1263–1265 (2011).
17. R. Romero, J. Espinoza, J. P. Kusanovic, F. Gotsch, S. Hassan, O. Erez, T. Chaiworapongsa, M. Mazor, The preterm parturition syndrome. *BJOG* **113** (suppl. 3), 17–42 (2006).
18. I. Burd, B. Balakrishnan, S. Kannan, Models of fetal brain injury, intrauterine inflammation, and preterm birth. *Am. J. Reprod. Immunol.* **67**, 287–294 (2012).
19. I. Kyvernitakis, H. Maul, F. Bahlmann, Controversies about the secondary prevention of spontaneous preterm birth. *Geburtshilfe Frauenheilkd.* **78**, 585–595 (2018).
20. D. G. Kiefer, M. R. Peltier, S. M. Keeler, O. Rust, C. V. Ananth, A. M. Vintzileos, N. Hanna, Efficacy of midtrimester short cervix interventions is conditional on intraamniotic inflammation. *Am. J. Obstet. Gynecol.* **214**, 276.e1–276.e6 (2016).
21. S. P. Murphy, N. N. Hanna, L. D. Fast, S. K. Shaw, G. Berg, J. F. Padbury, R. Romero, S. Sharma, Evidence for participation of uterine natural killer cells in the mechanisms responsible for spontaneous preterm labor and delivery. *Am. J. Obstet. Gynecol.* **200**, 308.e1–308.e9 (2009).
22. N. M. Shah, P. F. Lai, N. Imami, M. R. Johnson, Progesterone-related immune modulation of pregnancy and labor. *Front. Endocrinol.* **10**, 198 (2019).
23. G. C. Di Renzo, I. Giardina, G. Clerici, E. Brillo, S. Gerli, Progesterone in normal and pathological pregnancy. *Horm. Mol. Biol. Clin. Investig.* **27**, 35–48 (2016).
24. J. R. Challis, C. J. Lockwood, L. Myatt, J. E. Norman, J. F. Strauss III, F. Petraglia, Inflammation and pregnancy. *Reprod. Sci.* **16**, 206–215 (2009).
25. D. Pieber, V. C. Allport, F. Hills, M. Johnson, P. R. Bennett, Interactions between progesterone receptor isoforms in myometrial cells in human labour. *Mol. Hum. Reprod.* **7**, 875–879 (2001).
26. T. Zakar, S. Mesiano, How does progesterone relax the uterus in pregnancy? *N. Engl. J. Med.* **364**, 972–973 (2011).
27. S. A. Mesiano, G. A. Peters, P. Amini, R. A. Wilson, G. P. Tochtrop, F. van Den Akker, Progestin therapy to prevent preterm birth: History and effectiveness of current strategies and development of novel approaches. *Placenta* **79**, 46–52 (2019).
28. L. Nadeem, O. Shynlova, E. Matysiak-Zablocki, S. Mesiano, X. Dong, S. Lye, Molecular evidence of functional progesterone withdrawal in human myometrium. *Nat. Commun.* **7**, 11565 (2016).
29. H. Tan, L. Yi, N. S. Rote, W. W. Hurd, S. Mesiano, Progesterone receptor-A and -B have opposite effects on proinflammatory gene expression in human myometrial cells: Implications for progesterone actions in human pregnancy and parturition. *J. Clin. Endocrinol. Metab.* **97**, E719–E730 (2012).
30. G. A. Peters, L. Yi, Y. Skomorovska-Prokvolit, B. Patel, P. Amini, H. Tan, S. Mesiano, Inflammatory stimuli increase progesterone receptor-a stability and transrepressive activity in myometrial cells. *Endocrinology* **158**, 158–169 (2017).
31. J. Lei, J. M. Rosenzweig, M. K. Mishra, W. Alshehri, F. Brancusi, M. McLane, A. Almalki, R. Bahabry, H. Arif, R. Rozzah, G. Alyousif, Y. Shabi, N. Alhehaily, W. Zhong, A. Facciabene, S. Kannan, R. M. Kannan, I. Burd, Maternal dendrimer-based therapy for inflammation-induced preterm birth and perinatal brain injury. *Sci. Rep.* **7**, 6106 (2017).
32. C. M. Novak, M. Ozen, M. McLane, S. Alqutub, J. Y. Lee, J. Lei, I. Burd, Progesterone improves perinatal neuromotor outcomes in a mouse model of intrauterine inflammation via immunomodulation of the placenta. *Am. J. Reprod. Immunol.* **79**, e12842 (2018).
33. M. A. Elovitz, C. Mrinalini, The use of progestational agents for preterm birth: Lessons from a mouse model. *Am. J. Obstet. Gynecol.* **195**, 1004–1010 (2006).
34. M. A. Elovitz, J. Gonzalez, Medroxyprogesterone acetate modulates the immune response in the uterus, cervix and placenta in a mouse model of preterm birth. *J. Matern. Fetal Neonatal Med.* **21**, 223–230 (2008).
35. M. A. Elovitz, Z. Wang, E. K. Chien, D. F. Rychlik, M. Phillippe, A new model for inflammation-induced preterm birth: The role of platelet-activating factor and Toll-like receptor-4. *Am. J. Pathol.* **163**, 2103–2111 (2003).
36. M. A. Elovitz, A. G. Brown, K. Breen, L. Anton, M. Maubert, I. Burd, Intrauterine inflammation, insufficient to induce parturition, still evokes fetal and neonatal brain injury. *Int. J. Dev. Neurosci.* **29**, 663–671 (2011).
37. M. Elovitz, Z. Wang, Medroxyprogesterone acetate, but not progesterone, protects against inflammation-induced parturition and intrauterine fetal demise. *Am. J. Obstet. Gynecol.* **190**, 693–701 (2004).
38. S. M. Yellon, C. A. Ebner, M. A. Elovitz, Medroxyprogesterone acetate modulates remodeling, immune cell census, and nerve fibers in the cervix of a mouse model for inflammation-induced preterm birth. *Reprod. Sci.* **16**, 257–264 (2009).
39. H. C. Zierden, J. I. Ortiz Ortiz, P. Dimitrion, V. Laney, S. Bensouda, N. M. Anders, M. Scardina, T. Hoang, B. M. Ronnett, J. Hanes, I. Burd, M. Mahendroo, L. M. Ensign, Characterization of an adapted murine model of intrauterine inflammation–induced preterm birth. *Am. J. Pathol.* **190**, 295–305 (2019).
40. S. K. Munro, M. D. Mitchell, A. P. Ponnampalam, Histone deacetylase inhibition by trichostatin A mitigates LPS induced TNFα and IL-10 production in human placental explants. *Placenta* **34**, 567–573 (2013).
41. M. D. Mitchell, Unique suppression of prostaglandin H synthase-2 expression by inhibition of histone deacetylation, specifically in human amnion but not adjacent choriodecidua. *Mol. Biol. Cell* **17**, 549–553 (2006).
42. R. J. Phillips, A. J. Tyson-Capper Née Pollard, J. Bailey, S. C. Robson, G. N. Europe-Finner, Regulation of expression of the chorionic gonadotropin/luteinizing hormone receptor gene in the human myometrium: Involvement of specificity protein-1 (Sp1), Sp3, Sp4, Sp-like proteins, and histone deacetylases. *J. Clin. Endocrinol. Metab.* **90**, 3479–3490 (2005).
43. J. C. Condon, P. Jeyasuria, J. M. Faust, J. W. Wilson, C. R. Mendelson, A decline in the levels of progesterone receptor coactivators in the pregnant uterus at term may antagonize progesterone receptor function and contribute to the initiation of parturition. *Proc. Natl. Acad. Sci. U.S.A.* **100**, 9518–9523 (2003).
44. G. P. Wagner, M. C. Nnamani, A. R. Chavan, J. Maziarz, S. Protopapas, J. Condon, R. Romero, Evolution of gene expression in the uterine cervix related to steroid signaling: Conserved features in the regulation of cervical ripening. *Sci. Rep.* **7**, 4439 (2017).
45. A. H. Kishore, H. Liang, M. Kanchwala, C. Xing, T. Ganesh, Y. Akgul, B. Posner, J. M. Ready, S. D. Markowitz, R. A. Word, Prostaglandin dehydrogenase is a target for successful induction of cervical ripening. *Proc. Natl. Acad. Sci. U.S.A.* **114**, E6427–E6436 (2017).
46. C. S. Dezzutti, E. R. Brown, B. Moncla, J. Russo, M. Cost, L. Wang, K. Uranker, R. P. Kunjara Na Ayudhya, K. Pryke, J. Pickett, M. A. Leblanc, L. C. Rohan, Is wetter better? An evaluation of over-the-counter personal lubricants for safety and anti-HIV-1 activity. *PLOS ONE* **7**, e48328 (2012).
47. M. Ilicic, T. Zakar, J. W. Paul, Modulation of progesterone receptor isoform expression in pregnant human myometrium. *Biomed. Res. Int.* **2017**, 4589214 (2017).
48. J. E. Le Belle, J. Sperry, A. Ngo, Y. Ghochani, D. R. Laks, M. López-Aranda, A. J. Silva, H. I. Kornblum, Maternal inflammation contributes to brain overgrowth and autism-associated behaviors through altered redox signaling in stem and progenitor cells. *Stem Cell Rep.* **3**, 725–734 (2014).
49. C. R. Laboratories, *NDA 20-756 for Crinone (8% Progesterone Gel for Vaginal Administration)* (1997).
50. L. Sanderson, G. W. Taylor, E. O. Aboagye, J. P. Alao, J. R. Latigo, R. C. Coombes, D. M. Vigushin, Plasma pharmacokinetics and metabolism of the histone deacetylase inhibitor trichostatin a after intraperitoneal administration to mice. *Drug Metab. Dispos.* **32**, 1132–1138 (2004).
51. P. Mittal, R. Romero, A. L. Tarca, J. Gonzalez, S. Draghici, Y. Xu, Z. Dong, C. L. Nhan-Chang, T. Chaiworapongsa, S. Lye, J. P. Kusanovic, L. Lipovich, S. Mazaki-Tovi, S. S. Hassan, S. Mesiano, C. J. Kim, Characterization of the myometrial transcriptome and biological pathways of spontaneous human labor at term. *J. Perinat. Med.* **38**, 617–643 (2010).
52. O. Shynlova, T. Nedd-Roderique, Y. Li, A. Dorogin, S. J. Lye, Myometrial immune cells contribute to term parturition, preterm labour and post-partum involution in mice. *J. Cell. Mol. Med.* **17**, 90–102 (2013).
53. D. A. MacIntyre, Y. S. Lee, R. Migale, B. R. Herbert, S. N. Waddington, D. Peebles, H. Hagberg, M. R. Johnson, P. R. Bennett, Activator protein 1 is a key terminal mediator of inflammation-induced preterm labor in mice. *FASEB J.* **28**, 2358–2368 (2014).
54. C. L. Tower, S. Lui, R. L. Jones, Are chemokines therapeutic targets for the prevention of preterm labor? *Immunotherapy* **6**, 901–904 (2014).
55. S. S. Hassan, R. Romero, A. L. Tarca, C. L. Nhan-Chang, E. Vaisbuch, O. Erez, P. Mittal, J. P. Kusanovic, S. Mazaki-Tovi, L. Yeo, S. Draghici, J. S. Kim, N. Uldbjerg, C. J. Kim, The transcriptome of cervical ripening in human pregnancy before the onset of labor at

term: Identification of novel molecular functions involved in this process. *J. Matern. Fetal Neonatal Med.* **22**, 1183–1193 (2009).
56. J. A. Keelan, M. Blumenstein, R. J. Helliwell, T. A. Sato, K. W. Marvin, M. D. Mitchell, Cytokines, prostaglandins and parturition—A review. *Placenta* **24** (suppl. A), S33–S46 (2003).
57. N. E. Renthal, C. C. Chen, K. C. Williams, R. D. Gerard, J. Prange-Kiel, C. R. Mendelson, miR-200 family and targets, ZEB1 and ZEB2, modulate uterine quiescence and contractility during pregnancy and labor. *Proc. Natl. Acad. Sci. U.S.A.* **107**, 20828–20833 (2010).
58. R. Holt, B. C. Timmons, Y. Akgul, M. L. Akins, M. Mahendroo, The molecular mechanisms of cervical ripening differ between term and preterm birth. *Endocrinology* **152**, 1036–1046 (2011).
59. M. Ruscheinsky, C. De la Motte, M. Mahendroo, Hyaluronan and its binding proteins during cervical ripening and parturition: Dynamic changes in size, distribution and temporal sequence. *Matrix Biol.* **27**, 487–497 (2008).
60. J. Condon, S. Yin, B. Mayhew, R. A. Word, W. E. Wright, J. W. Shay, W. E. Rainey, Telomerase immortalization of human myometrial cells. *Biol. Reprod.* **67**, 506–514 (2002).
61. L. Nadeem, O. Shynlova, S. Mesiano, S. Lye, Progesterone via its type-A receptor promotes myometrial gap junction coupling. *Sci. Rep.* **7**, 13357 (2017).
62. W. S. Xu, R. B. Parmigiani, P. A. Marks, Histone deacetylase inhibitors: Molecular mechanisms of action. *Oncogene* **26**, 5541–5552 (2007).
63. H. J. Kim, S. C. Bae, Histone deacetylase inhibitors: Molecular mechanisms of action and clinical trials as anti-cancer drugs. *Am. J. Transl. Res.* **3**, 166–179 (2011).
64. P. Yeo, L. Xin, E. Goh, L. S. New, P. Zeng, X. Wu, P. Venkatesh, E. Kantharaj, Development and validation of high-performance liquid chromatography-tandem mass spectrometry assay for 6-(3-benzoyl-ureido)-hexanoic acid hydroxyamide, a novel HDAC inhibitor, in mouse plasma for pharmacokinetic studies. *Biomed. Chromatogr.* **21**, 184–189 (2007).
65. J. Diaz, S. Abiola, N. Kim, O. Avaritt, D. Flock, J. Yu, F. J. Northington, R. Chavez-Valdez, Therapeutic hypothermia provides variable protection against behavioral deficits after neonatal hypoxia-ischemia: A potential role for brain-derived neurotrophic factor. *Dev. Neurosci.* **39**, 257–272 (2017).
66. M. A. L. J. M. Hill, M. M. Stone, Developmental milestones in the newborn mouse. *Neuromethods* **39**, 17 (2008).
67. L. Prut, C. Belzung, The open field as a paradigm to measure the effects of drugs on anxiety-like behaviors: A review. *Eur. J. Pharmacol.* **463**, 3–33 (2003).
68. C. Belzung, G. Griebel, Measuring normal and pathological anxiety-like behaviour in mice: A review. *Behav. Brain Res.* **125**, 141–149 (2001).
69. L. W. Doyle, G. Victorian, Neonatal intensive care at borderline viability—Is it worth it? *Early Hum. Dev.* **80**, 103–113 (2004).
70. H. A. Frey, M. A. Klebanoff, The epidemiology, etiology, and costs of preterm birth. *Semin. Fetal Neonatal Med.* **21**, 68–73 (2016).
71. L. P. Bengtsson, *Brook Lodge Symposium: Progesterone* (Augusta, 1961).
72. R. J. Kuon, S.-Q. Shi, H. Maul, C. Sohn, J. Balducci, W. L. Maner, R. E. Garfield, Pharmacologic actions of progestins to inhibit cervical ripening and prevent delivery depend on their properties, the route of administration, and the vehicle. *Am. J. Obstet. Gynecol.* **202**, 455.e1–455.e9 (2010).
73. E. Krispin, E. Hadar, R. Chen, A. Wiznitzer, B. Kaplan, The association of different progesterone preparations with preterm birth prevention. *J. Matern. Fetal Neonatal Med.* **32**, 3452–3457 (2018).
74. L. M. Ensign, R. Cone, J. Hanes, Nanoparticle-based drug delivery to the vagina: A review. *J. Control. Release* **190**, 500–514 (2014).
75. W. C. Aird, Spatial and temporal dynamics of the endothelium. *J. Thromb. Haemost.* **3**, 1392–1406 (2005).
76. T. Levy, Y. Yairi, I. Bar-Hava, J. Shalev, R. Orvieto, Z. Ben-Rafael, Pharmacokinetics of the progesterone-containing vaginal tablet and its use in assisted reproduction. *Steroids* **65**, 645–649 (2000).
77. A. Tavaniotou, J. Smitz, C. Bourgain, P. Devroey, Comparison between different routes of progesterone administration as luteal phase support in infertility treatments. *Hum. Reprod. Update* **6**, 139–148 (2000).
78. G. Wu, J. Chen, X. Hu, H. Zhou, J. Liu, D. Lv, L. Wu, J. Shentu, Pharmacokinetic properties of three forms of vaginal progesterone administered in either single or multiple dose regimen in healthy post-menopausal chinese women. *Front. Pharmacol.* **8**, 212 (2017).
79. C. Nold, M. Maubert, L. Anton, S. Yellon, M. A. Elovitz, Prevention of preterm birth by progestational agents: What are the molecular mechanisms? *Am. J. Obstet. Gynecol.* **208**, 223.e1–223.e7 (2013).
80. M. Patki, K. Giusto, S. Gorasiya, S. E. Reznik, K. Patel, 17-α hydroxyprogesterone nanoemulsifying preconcentrate-loaded vaginal tablet: A novel non-invasive approach for the prevention of preterm birth. *Pharmaceutics* **11**, 335 (2019).
81. R. McCarthy, C. Martin-Fairey, D. K. Sojka, E. D. Herzog, E. S. Jungheim, M. J. Stout, J. C. Fay, M. Mahendroo, J. Reese, J. L. Herington, E. J. Plosa, E. L. Shelton, S. K. England, Mouse models of preterm birth: Suggested assessment and reporting guidelines. *Biol. Reprod.* **99**, 922–937 (2018).
82. M. Weatherborn, S. Mesiano, Rationale for current and future progestin-based therapies to prevent preterm birth. *Best Pract. Res. Clin. Obstet. Gynaecol.* **52**, 114–125 (2018).
83. J. G. Fleming, T. E. Spencer, S. H. Safe, F. W. Bazer, Estrogen regulates transcription of the ovine oxytocin receptor gene through GC-rich SP1 promoter elements. *Endocrinology* **147**, 899–911 (2006).
84. M. Ilicic, T. Zakar, J. W. Paul, Epigenetic regulation of progesterone receptors and the onset of labour. *Reprod. Fertil. Dev.* **31**, 1035–1048 (2019).
85. T. M. Lindstrom, A. R. Mohan, M. R. Johnson, P. R. Bennett, Histone deacetylase inhibitors exert time-dependent effects on nuclear factor-kappaB but consistently suppress the expression of proinflammatory genes in human myometrial cells. *Mol. Pharmacol.* **74**, 109–121 (2008).
86. T. Kawanai, Y. Ago, R. Watanabe, A. Inoue, A. Taruta, Y. Onaka, S. Hasebe, H. Hashimoto, T. Matsuda, K. Takuma, Prenatal exposure to histone deacetylase inhibitors affects gene expression of autism-related molecules and delays neuronal maturation. *Neurochem. Res.* **41**, 2574–2584 (2016).
87. C. Nicolini, M. Fahnestock, The valproic acid-induced rodent model of autism. *Exp. Neurol.* **299**, 217–227 (2018).
88. S. Huang, W. Dong, Z. Jiao, J. Liu, K. Li, H. Wang, D. Xu, Prenatal dexamethasone exposure induced alterations in neurobehavior and hippocampal glutamatergic system balance in female rat offspring. *Toxicol. Sci.* **171**, 369–384 (2019).
89. J. E. Norman, N. Marlow, C. M. Messow, A. Shennan, P. R. Bennett, S. Thornton, S. C. Robson, A. McConnachie, S. Petrou, N. J. Sebire, T. Lavender, S. Whyte, J. Norrie; OPPTIMUM Study Group, Vaginal progesterone prophylaxis for preterm birth (the OPPTIMUM study): A multicentre, randomised, double-blind trial. *Lancet* **387**, 2106–2116 (2016).
90. A. A. Date, G. Halpert, T. Babu, J. Ortiz, P. Kanvinde, P. Dimitrion, J. Narayan, H. Zierden, K. Betageri, O. Musmanno, H. Wiegand, X. Huang, S. Gumber, J. Hanes, L. M. Ensign, Mucus-penetrating budesonide nanosuspension enema for local treatment of inflammatory bowel disease. *Biomaterials* **185**, 97–105 (2018).
91. AMAG Pharmaceuticals Inc., "Makena" (2018); www.accessdata.fda.gov/drugsatfda_docs/nda/2011/021945_makena_toc.cfm.
92. A. B. Nair, S. Jacob, A simple practice guide for dose conversion between animals and human. *J. Basic Clin. Pharm.* **7**, 27–31 (2016).
93. G. Elaut, G. Laus, E. Alexandre, L. Richert, P. Bachellier, D. Tourwe, V. Rogiers, T. Vanhaecke, A metabolic screening study of trichostatin A (TSA) and TSA-like histone deacetylase inhibitors in rat and human primary hepatocyte cultures. *J. Pharmacol. Exp. Ther.* **321**, 400–408 (2007).
94. A. C. Heuerman, T. T. Hollinger, R. Menon, S. Mesiano, S. M. Yellon, Cervix stromal cells and the progesterone receptor a isoform mediate effects of progesterone for prepartum remodeling. *Reprod. Sci.* **26**, 690–696 (2019).
95. E. Dallot, M. Pouchelet, N. Gouhier, D. Cabrol, F. Ferré, M. Breuiller-Fouché, Contraction of cultured human uterine smooth muscle cells after stimulation with endothelin-1. *Biol. Reprod.* **68**, 937–942 (2003).
96. S. Makieva, L. J. Hutchinson, S. P. Rajagopal, S. F. Rinaldi, P. Brown, P. T. Saunders, J. E. Norman, Androgen-induced relaxation of uterine myocytes is mediated by blockade of both Ca^{2+} flux and MLC phosphorylation. *J. Clin. Endocrinol. Metab.* **101**, 1055–1065 (2016).
97. A. K. Boyle, S. F. Rinaldi, A. G. Rossi, P. T. K. Saunders, J. E. Norman, Repurposing simvastatin as a therapy for preterm labor: Evidence from preclinical models. *FASEB J.* **33**, 2743–2758 (2019).

Acknowledgments: We acknowledge the JHMI animal husbandry staff for tending to our animals. We would like to thank N. Hernández and B. Zak for help in collecting tissue samples and performing behavior analysis. We acknowledge and appreciate input from G. Halpert and L. McCrea regarding experiment design, and we thank S. Zierden for productive scientific conversations and assistance with final edits. **Funding:** The work was primarily supported by the Burroughs Wellcome Preterm Birth Initiative, grant 1015020 awarded to L.M.E.; H.C.Z. was supported by an NSF GRFP Fellowship (DGE-1746891); and K.D. was supported by a Hartwell Foundation Postdoctoral Fellowship. G.W. was supported by the National Cancer Institute, grant number U54-CA209992, and by the John Templeton Foundation, grant number 61329. Pharmacokinetic studies were supported by the Analytical Pharmacology Core of the Sidney Kimmel Comprehensive Cancer Center at Johns Hopkins (NIH grants P30CA006973 and UL1TR003098 and the Shared Instrument Grant S10RR026824). The project described was also supported by grant number UL1TR003098 from the National Center for Advancing Translational Sciences (NCATS), a component of the NIH, and the NIH Roadmap for Medical Research. Its contents are solely the responsibility of the authors and do not necessarily represent the official view of the NCATS or NIH. **Author contributions:** H.C.Z., K.D., N.M.A., M.M., S.M., I.B., G.W., J.H., and L.M.E. contributed to the experimental design. H.C.Z., K.D., J.I.O., N.M.A., and L.M.E. contributed to writing sections of the manuscript. H.C.Z. and G.L. performed the NS formulation and characterization. J.I.O. performed all surgeries. H.C.Z., J.I.O., V.L., and S.B. collected tissue samples and performed the RNA extraction. H.C.Z., J.Y., G.L., and P.D.

performed RT-qPCR experiments. J.Y. performed cell culture experiments. G.L. and A.B. performed the behavior analysis on pups. N.M.A. and M.S. developed drug detection methods and analyzed PK samples. H.C.Z., J.I.O., K.D., N.M.A., S.M., G.W., J.H., and L.M.E. contributed to data analysis and interpretation. All authors contributed to the manuscript, assisted in revisions, read, and approved the submitted version. **Competing interests:** The mucus-penetrating particle technology is licensed and in clinical development for ocular indications by Kala Pharmaceuticals. J.H. is a founder of Kala Pharmaceuticals and serves as a consultant. J.H. and Johns Hopkins own company stock. Under a licensing agreement between Kala Pharmaceuticals and the Johns Hopkins University, L.M.E., J.H., and the University are entitled to royalty distributions related to the technology. These arrangements have been reviewed and approved by the Johns Hopkins University in accordance with its conflict of interest policies. All other authors declare that they have no competing interests. **Data and materials availability:** All data associated with this study are present in the paper or the Supplementary Materials.

Submitted 5 May 2020
Accepted 13 October 2020
Published 13 January 2021
10.1126/scitranslmed.abc6245

Citation: H. C. Zierden, J. I. Ortiz, K. DeLong, J. Yu, G. Li, P. Dimitrion, S. Bensouda, V. Laney, A. Bailey, N. M. Anders, M. Scardina, M. Mahendroo, S. Mesiano, I. Burd, G. Wagner, J. Hanes, L. M. Ensign, Enhanced drug delivery to the reproductive tract using nanomedicine reveals therapeutic options for prevention of preterm birth. *Sci. Transl. Med.* **13**, eabc6245 (2021).

Science Translational Medicine

Enhanced drug delivery to the reproductive tract using nanomedicine reveals therapeutic options for prevention of preterm birth

Hannah C. ZierdenJairo I. OrtizKevin DeLongJingqi YuGaoshan LiPeter DimitrionSabrine BensoudaVictoria LaneyAnna BaileyNicole M. AndersMorgan ScardinaMala MahendrooSam MesianoIrina BurdGunter WagnerJustin HanesLaura M. Ensign

Sci. Transl. Med., 13 (576), eabc6245. • DOI: 10.1126/scitranslmed.abc6245

Drug delivery to delay delivery

Preterm birth, often caused by inflammation, is a major contributor to infant morbidity and mortality. It often cannot be predicted, but even for women who are known to be at risk of preterm delivery, there is no currently approved intervention to prevent it, although progesterone-based interventions are sometimes attempted. To improve access of treatments to the appropriate tissues for preventing preterm delivery, Zierden *et al.* designed a mucoinert nanosuspension to optimize vaginal dosing of therapeutics. The authors demonstrated the effectiveness of their approach in mouse models using histone deacetylase inhibitors with and without progesterone. Their approach improved the rates of full-term delivery of neurotypical pups.

Science Translational Medicine (ISSN 1946-6242) is published by the American Association for the Advancement of Science. 1200 New York Avenue NW, Washington, DC 20005. The title *Science Translational Medicine* is a registered trademark of AAAS.